TECHNISCHE
UNIVERSITÄT
WIEN
Vienna University of Technology

DIPLOMARBEIT

Formation and Theoretical Investigations of Inorganic-Organic Hybrid Materials via the Interaction of Bidentate Ligands with Metals

Institut für Materialchemie
Technische Universität Wien

unter der Anleitung von
Prof. Ulrich Schubert
Prof. Guido Kickelbick

durch
Thomas Gallauner
Gerasdorferstraße 55/9/3
1210 Wien

Wien, 2004

Contents

Part I

Preface

Acknowledgment

I want to thank *Prof. Ulrich Schubert*, who gave me the possibility to carry out this degree dissertation in his working group, and *Prof. Guido Kickelbick* for his support and guidance during this work.

I also want to thank *Dr. Dietmar Sturmayr* for his introduction and advice in computational chemistry.

Furthermore I want to thank *Dr. Michael Puchberger* for his support in NMR spectroscopy and his aid in my practical work.

Special thanks are addressed to my friends *Eva-Maria Lichtenberg* and *Gregor Tatschl* for proofreading this work. I am very grateful for our close friendship.

Finally I want to thank my parents for their continuous support, which allowed me to follow my interests and gave me the opportunity to study.

Abstract

This work deals with the synthesis, characterization and application of new β-dicarbonyl based ligands with the advantage of forming 3D coordinating hybrid materials. In the first part ligands that are able to form structured networks containing two coordinating centers were discussed. The investigated ligands were 2,3-diacetylhexan-2,5-dione, tetrabenzoylethane and tetramethylethane-1,1,2,2-tetracarboxylate. Those dimer β-diketones were synthesized by a dimerization of acetylacetone, dibenzoylethane and dimethyl malonate, characterized by NMR- and solid state ATR-IR-spectroscopy and single crystal X-ray diffraction. The obtained ligands were coordinated to metal ions that are able to form various coordination environments. These investigations were aided by *ab initio* calculations to obtain energetical and electronical properties of the discussed structures and were compared to the experimental results. Although no structures providing a long-range crystalline order could be obtained the coordination of this novel systems could be well interpreted and characterized, which was also proven by *ab initio* calculations.

In a second part a theoretical study on halogenated pentane-2,4-dione molecules was carried out to prove their ability to act as initiating molecules for atom transfer radical polymerization (ATRP) by a homogenous cleavage of the carbon-halogen bond. The obtained results were compared to those of regular initiating molecules. Furthermore the electronical and structural properties of the cleaved initiators were investigated to obtain information about the initiation process.

Kurzfassung der Arbeit

Diese Arbeit behandelt die Darstellung, Untersuchung und Anwendung neuartiger β-Dicarbonyl-Liganden als Vorstufe zur Bildung dreidimensional koordinierter metallorganischer Hybridstrukturen. Die im ersten Teil dieser Arbeit diskutierten Liganden enthalten zwei potentielle Koordinationszentren mit der Möglichkeit räumlich geordnete molekulare Strukturen aufzubauen. Bei den untersuchten Liganden handelt es sich um 2,3-Diacetylhexan-2,5-dion, 2,3-Dibenzoyl-1,4-diphenylbutan-1,4-dion und Tetramethylethan-1,1,2,2-tetracarboxylat, welche durch eine Dimerisierungsreaktion aus Acetylaceton, Dibenzoylmethan und Dimethylmalonat hergestellt und mittels NMR- und ATR-FT-IR-Spektorskopie untersucht wurden. Die erhaltenen Liganden wurden an unterschiedliche Metallionen koordiniert, woraus unterschiedliche Koordinationsgeometrien resultierten. Zusätzlich zu diese Untersuchungen wurden *ab inito* Berechnungen durchgeführt um genauere Information über Stabilität und elektronische Charakteristika zu erhalten. Obwohl keine kristallinen Systeme erhalten werden konnten, war es möglich diese neuartigen Strukturen mit Hilfe theoretischer Betrachtungen eingehend zu untersuchen und zu charakterisieren.

Der zweite Teil dieser Arbeit behandelt halogenierte Acetylacetone als mögliche Initiatoren für die Atom-Transfer-Radikal-Polymerisation (ATRP), welche zusätzlich an Metall-Ionen koordinieren können. In einer theoretischen Studie wurde die homolytische Spaltung der Kohlenstoff-Halogen-Bindung energetisch untersucht. Die erhaltenen Ergebnisse wurden mit einer Gruppe üblicher ATRP-Initiatoren verglichen und alle resultierenden Radikale elektronisch untersucht um weitere Einblicke in die Startreaktion der Polymerisation zu erhalten.

Introduction

In recent years the construction of extended ordered solids from molecular building blocks by supramolecular approaches and the combination of inorganic and organic moieties in one material gained great interest due to the advantages it offers for the design of materials such as excellent control over the structure and functionality of the prepared systems [1, 2, 3].

Two different approaches for the preparation of such complex materials are considered in this work. The first one uses molecular linkers containing coordination sites that allow the formation of extended 3D networks via the coordination to metals. The other one is based on compounds that allow a coordination to a metal and at the same time the initiation of a polymerization.

The basic step for the construction of extended solids is based on the coordination of an organic ligands, which have separated groups that allow the coordination to two or more metal ions at the same time. Typical examples of such poly topic linkers are 4,4'-bipyridine, 1,4-benzenedicarboxylate and 1,4-azodibenzoate, which can coordinate to two metal ions [1]. For higher coordination numbers 1,3,5-benzenetricarboxylate and 1,3,5,7-adamantanetetracarboxylate were used (figure 1) [1]. Depending on the coordination number and the molecular structure of the linker a large variety of 3D structures is possible. The two main groups that are formed are either discrete supramolecular polygons and polyhedra or extended frameworks. Figure 2 shows a theoretical consideration of two different structures which may result from the reaction of a linker with a metal of the coordination number three (*a*) and four (*b*) [4]. In the other case instead of discrete supramolecular objects a continuous network is formed. By the combination of a linker with two

mono- or multidentate coordination centers and a metal of the coordination number two concerning the linker a linear coordination polymer is expected. In every other combination of linker and metal where the number of connection bonds exceeds two a three dimensional structure is formed. An example is given in figure 3 where 4,4'-bipyridine as linker interacts with a metal ion forming a tetrahedral coordinated substructure, which is also called a secondary building unit (SBU) [1]. A further linkage of these substructures builds up a regular expanded framework. This synthetic strategy offers a completely new field of partly crystalline solids, because of the combination of metals and organic molecules which form periodic structures based on coor-

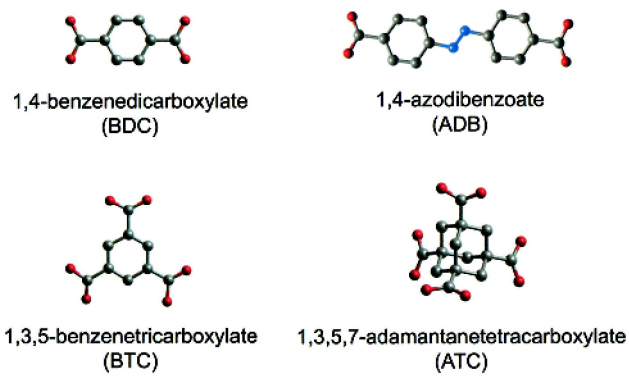

Figure 1: Poly topic organic linkers

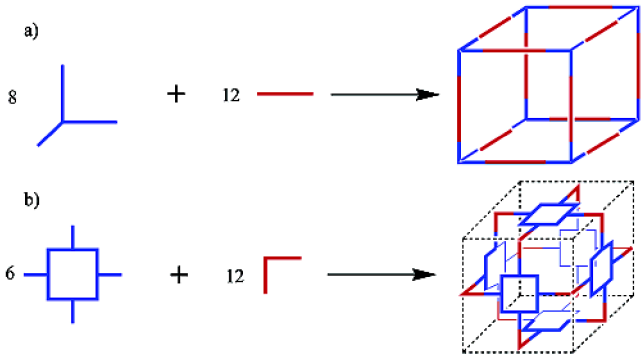

Figure 2: Coordination Cages

dination interaction. Another effect achieved by the use of linkers is the high porosity of the structure. As an example the resulting three dimensional net-

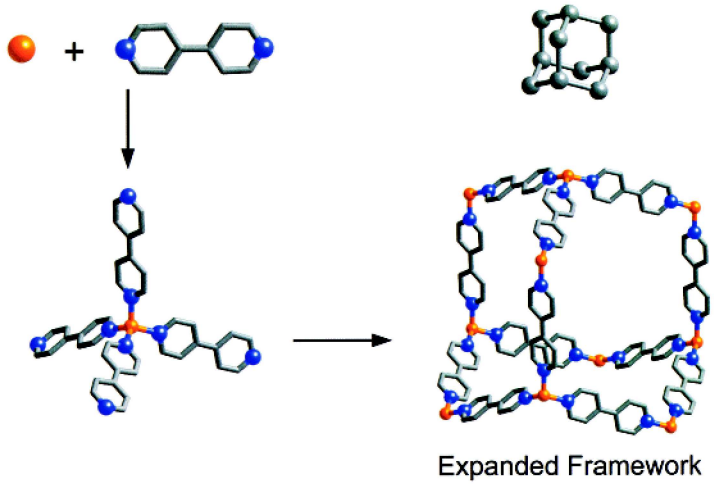

Figure 3: Coordination Networks

work achieved by the reaction of zinc acetate with 1,4-benzenedicarboxylate (BDC)[5, 6] is shown in figure 4. The structure formed is a simple cubic network, containing the primary building unit $Zn_4O(BDC)_3.(DMF)_8$ (a), where the carbon atoms are the vertices of an octahedron surrounding the Zn-atoms (b), building up a primitive cubic lattice. The substance obtained (c) is one of the most porous known to date.

Usually the bridges between the metal centers are well defined molecules. If polymers are used more irregular systems will be obtained. Two different materials can be envisioned, either the polymers are attached to two or more metal centers and form bridges between them, or the polymer chains are attached by only one site to the metal atom. Both material types are often called hybrid materials [7, 8, 9]. In recent years special attention was drawn to the controlled formation of such materials. For a high control of the structural properties of these materials it is necessary to apply controlled polymerization reactions, such as ATRP [10]. Because of its controlled character ATRP allows for the preparation of well-defined polymers through the mini-

mization of irreversible chain-transfer and chain-termination reactions. If the initiation process is complete and the exchange between species of various reactivities is fast, the final average molecular weight of the polymer is determined by the initial monomer-to-initiator ratio while maintaining a narrow molecular weight distribution, which is usually below 1.5. Contrary to other controlled radical polymerization techniques, such as RAFT [11, 12, 13, 14] or nitroxide mediated radical polymerization [15, 16, 17] ATRP allows the use of many different initiator systems and the production of a plethora of different polymer topologies and compositions.

A typical ATRP requires a monomer, a catalyst and an initiator. In the case of the copper mediated ATRP the catalytic active species is a complex of a copper(I) halide with an amine ligand. The metal catalyst undergoes a one-electron reaction with concomitant abstraction of a halogen atom from a

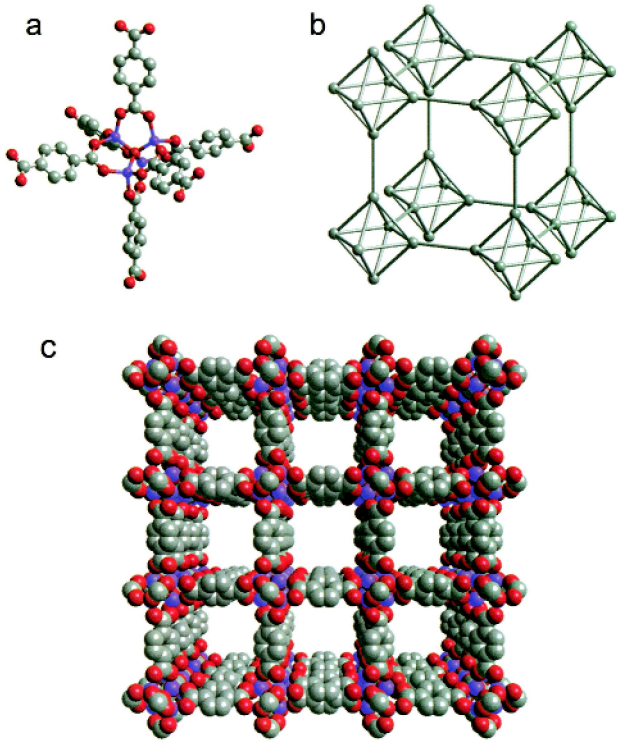

Figure 4: Porous Network

substrate, creating an organic radical and a copper(II) complex. The resulting radicals can add to an unsaturated compound generating a new radical. Repeating this cycle results in a chain-growth polymerization. Termination of the chains by radical coupling may occur as a side reaction during polymerization but due to the very low concentration of radicals formed in the equilibrium the probability of such an event is decreased. A scheme of the general mechanism of ATRP [18] is shown in figure 5.

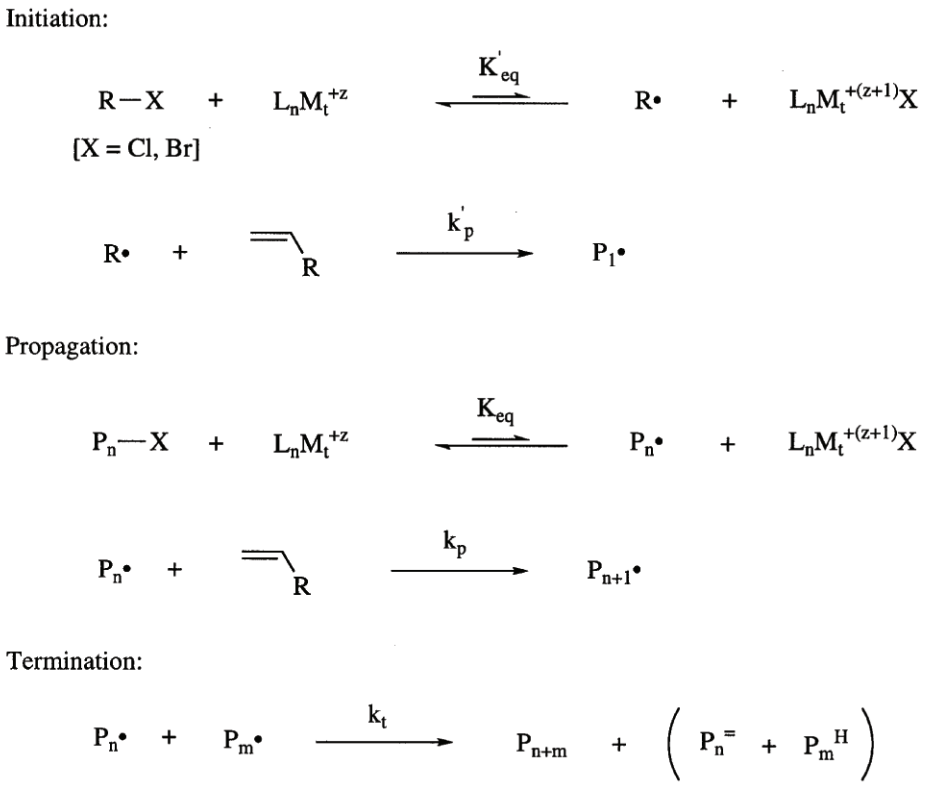

Figure 5: The general mechanism of ATRP [18]

Many different interesting morphologies can be obtained via controlled radical polymerization technique. One of them are star-like structures with a metal containing core and a polymer shell [19, 20, 21]. One possibility to achieve the formation of star polymers is the coordination of ATRP initiators to metals, which requires the combination of coordination groups and

initiating groups in one molecule. Either single metal ions or metal containing clusters can be used as multifunctional initiators for such morphologies. For example organically modified oxometallate clusters were used resulting in the formation of so called core-shell nanoparticles [19, 20]. The initiators able forming such a core particle discussed in this work are 3-chloro-2,4-pentandione and 3-bromo-2,4-pentandione.

Due to great development in recent years theoretical chemistry became a very powerful tool to support experimental work. *Ab initio* and particulars density functional theory calculations allow for the interpretation and understanding of experimentally obtained results in a much better way. In theoretical chemistry three main approaches exist for describing and calculating molecular structures. The first two approaches are force field theory and semiempirical methods. These models are fast and easy to calculate but do not provide the desired precision of the obtained results, especially for transition metal systems. The third method, which is the method predominantly used in this work, are so called *ab initio* calculations. This theory provides a high accuracy of the results and as a further advantage it does not need any experimental data but only fundamental constants as parameters. But in comparison to force field theory and semiempirical methods it shows a far higher demand in computational resources. The *ab initio* calculations based on density functional theory uses itself two different approaches to describe molecular systems. The first one was developed for discrete molecular structures. In this case the Schrödingers equation (equation 1) - describing

$$\left(\frac{-h^2}{8\pi^2 m}\nabla^2 + V\right)\psi(\vec{r},t) = \frac{\hat{\imath}h}{2\pi}\frac{\partial\psi(\vec{r},t)}{\partial t} \tag{1}$$

an electron wavefunction ψ with m as the mass of the particle, h the Planck's constant and V as the potential - is approximated by the combination of atomic orbitals (AO's) which are combined to molecular orbitals (MO's) (equation 2)

$$\psi(\vec{r}) = \phi_1(\vec{r}_1)\phi_2(\vec{r}_2)\ldots\phi_n(\vec{r}_n) \tag{2}$$

that describe the electronic state of a molecule. The most commonly applied mathematical function to describe atomic orbitals are of the Gaussian type.

The resulting orbitals are therefore called Gaussian type orbitals (GTO's) (equation 3).

$$\chi_{\xi,n,l,m}(r,\theta,\varphi) = NY_{l,m}(\theta,\varphi)r^{2n-2-l}e^{-\xi r^2} \tag{3}$$

The reason for their use is that these mathematical functions allow fast computational algorithms. A completely different approach, which was derived in solid state physics, develops from periodic boundary conditions. In such systems the solution of the Schrödingers Equation leads to *plane waves*. A generalized form of such a wavefunction is shown in equation 4,

$$f(\vec{r}) = \Omega^{-\frac{1}{2}}e^{\hat{i}\vec{k}\vec{r}} \tag{4}$$

where $\vec{k}$ is the propagation direction of the plane waves and Ω the corresponding volume of periodicity. The great advantage of this theory is that it also allows the theoretical investigation of discrete molecular structures with less computational afford by increasing the volume of periodicity in that way that the influence by interaction of this neighbor molecules can be neglected. This allows the characterization of more complex structures still providing a high accuracy of the obtained results. A disadvantage of this theory is that it allows only the characterization of closed-shell systems, which is the reason that for radical compounds MO theory had to be used. A very functional and widely used software package that uses atomical orbitals theory is GAUSSIAN98 [22]. As expressed in the name it uses Gaussian type orbitals as basis for calculations. The software applied for plane waves theory, which allowed the characterization of larger systems, is CPMD (Car Parinello Molecular Dynamics) [23]. This program also allows studies using molecular dynamics, but such studies were not carried out in this work.

Part II

Research Objectives

This work focuses on the synthesis and characterization of inorganic-organic hybrid materials based on the interaction of bidentate ligands with metals. Concomitantly the experimental work is extended by theoretical considerations of the expected and obtained results by *ab initio* calculations. In detail the following studies were carried out:

- The synthesis and characterization of dimer β-diketones suitable as ligands for the formation of inorganic-organic structured networks. A study of the effect of different substituents at the β-diketones on sterical and electronical properties was carried out. The investigations were aided by the application of DFT calculations for theoretical considerations.

- Formation and characterization of molecular networks by application of the bidentate ligands to different metal ions. The obtained results were compared to theoretically predicted values of calculated model compounds.

- Theoretical investigations of initiators for ATRP, which were compared to experimentally gained data and furthermore determination of the electronical characteristics of the respective radicals.

- A theoretical study of ATPR initiators based on β-diketones investigating their structure, their behavior of cleavage and also the characterization of the obtained radicals was carried out.

Part III

Results and Discussion

Chapter 1

Synthesis, Characterization and Theoretical Investigations of β-Diketones

This chapter deals with the synthesis and characterization of the different β-diketones with the ability to form three dimensional inorganic-organic hybrid networks by coordination to different metals. This practical work was compared to results of *ab initio* calculations using Hartree-Fock and DFT approaches. Those calculations were carried out with the software packages GAUSSIAN98 [22] and CPMD [23]. GAUSSIAN98 is a commonly applied program that, depending on the calculated systems, reaches high accuracy for geometry optimization, vibrational analysis and prediction of magnetical shifts for ^{1}H and ^{13}C NMR spectroscopy using Gaussian type orbitals. The disadvantage of the use of Gaussian type molecular orbitals is the high demand in computational resources for larger systems, such as the β-diketones and metal complexes discussed in this work, even if simplified molecules were calculated. For the other systems the software package CPMD, which is based on plane waves theory, was used to optimize the geometry and perform prediction of IR absorption bands and magnetical shifts. The theoretical investigations on 2,3-diacetylhexane-2,5-dione were used to study the electronical properties of this class of compounds and to perform a case study

to test the software package CPMD for the above mentioned systems. This was necessary for the interpretation of the results of the larger systems, which could not be calculated with GAUSSIAN98. CPMD calculations were carried out for the larger compounds providing a better ratio between calculation time and result quality, discussed later in this chapter.

1.1 2,3-Diacetylhexane-2,5-dione

1.1.1 Synthesis

The synthesis of this dimer β-diketone can be achieved by applying different approaches, for example chemical or electrochemical oxidative dimerization of acetylacetone by cerium(IV) salts [24]. This method provides a high yield of the product but it is cost intensive and difficult to apply due to the use of cerium(IV)salts and the apparatuses necessary for the electrochemical reaction.In this work 3,4-diacetylhexane-2,5-dione *(1)* was synthesized in a two step reaction [25, 26]. First pentane-2,5-dione was added at room temperature to a diethyl ether slurry of sodium hydride to form the sodium salt by deprotonation. Afterwards iodine was added and by radical coupling the dimer was formed as a white solid in 35% yield.

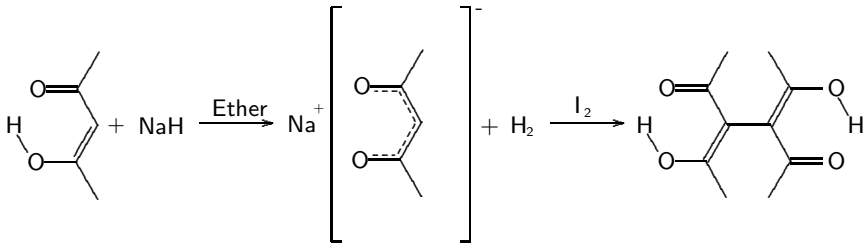

Figure 1.1: Synthesis of 3,4-diacetylhexane-2,5-dione

1.1.2 Characterization

NMR Spectroscopy

^{1}H NMR spectroscopy in $CDCl_3$ showed that the molecule exists exclusively in the dienole form because only singlet protons of the methyl groups at 2.0 *ppm* and those of the hydroxy group at 16.8 *ppm* could be found. The formation of an enole is also supported by the ^{13}C spectrum, which shows only two signals for the carbons of the methyl groups at 23.6 *ppm*, the carbons in positions (3) and (3A) at 108.1 *ppm* and the enole carbon at 192.7 *ppm* (for details see table 1.6 and 1.7). These observations are contrary to that found in literature [27] for the same molecule. In this previous work only a ^{1}H NMR study in $CDCl_3$ was reported. Also a singlet at 2.0 *ppm* for the methyl groups was observed, but instead of the hydroxy signal of the dienole tautomer a signal at 6.1 *ppm* was reported indicating a hydrogen localized at the tertiary carbons. The reason for this different results is unclear, in particular because the same conditions were used in the two studies.

IR Spectroscopy

The interpretation of the obtained NMR spectra was confirmed by the solid state ATR-IR spectrum also showing no carbonyl functionalities. The absorption band for the O-H stretching at 3005 cm^{-1} is very weak which may also result from the exchange of the hydrogens between the two oxygen atoms. Again the literature[27] values do not go along with that because a sharp absorption band at 1726 cm^{-1} typical for carbonyl bonds was reported. So the most obvious reason could be a contamination that influences the tautomerism. Those values were compared to the spectrum of acetylacetone, which is a mixture of both tautomers. The experimental obtained wavenumbers and the values provided by literature are in good agreement with acetylacetone [28], that shows the functionalities of an enole with absorption bonds at 1250, 1360, 1620 and 3000 cm^{-1} values of a hydroxy functionality and further absorption bonds at 1710 and 1725 cm^{-1} of a carboxy group. Obviously, although both molecules, the one described in this work and the one described in literature, have the same structure they show different tautomers.

Single Crystal X-Ray Diffraction Analysis

3,4-Diacetylhexane-2,5-dione was recrystallized from acetonitrile and crystals usable for single crystal X-ray diffraction were formed. The molecular structure obtained is shown in figure 1.2 and selected bond lengths and angles are shown in table 1.5. The most noticeable structural feature is the stabilization of the enole conformation in both β-diketone groups by the H-bridge which results in a nearly planar six membered ring, in which every carbon atom shows sp^2 hybridization. Obviously no conjugation between the delocalized electron systems occur because the two planarized β-diketone groups stand perpendicular to each other with a C(2)-C(3)-C(3A)-C(4A) torsion angle of 90.3° (figure 1.5). The distance between the atoms C(2) and C(3) (1.398 Å) lies between that of a single and a double bond as expected due to mesomery. This gives also an explanation of the extremely high shift for the enolic hydroxy proton in ^{1}H NMR because the magnetic field is actually influenced by delocalized electrons and those of two oxygen atoms. The distance between atom C(3) and C(3A) is 1.494 Å indicating a single bond, which is also supported by the obtained dihedral angle along that axis. The packing

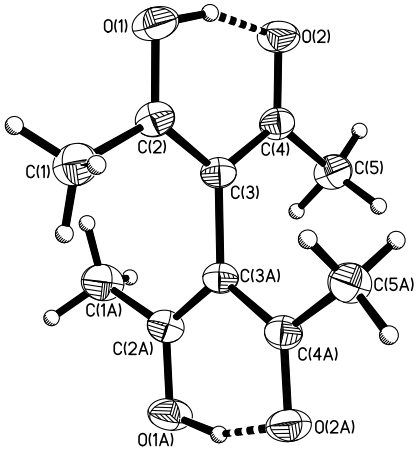

Figure 1.2: ORTEP plot of 3,4-diacetylhexane-2,5-dione

of the crystal structure along [100] is shown in figure 1.3. It reveals clearly the torsion angle of nearly 90 degrees along the C(3)-C(3A) bond and the stacking of the molecules. Beside the intramolecular H-bridges there are obviously no intermolecular H-bridging interactions of the discrete molecules in the crystal packing.

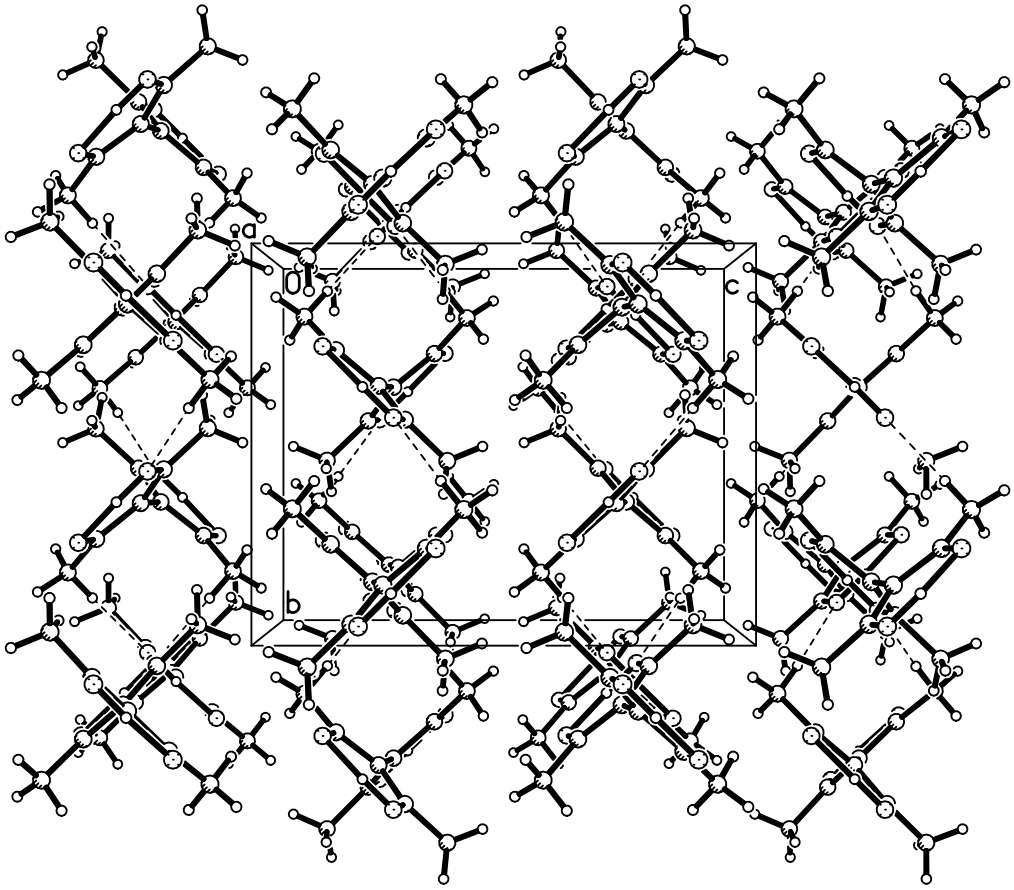

Figure 1.3: Crystal packing of 2,3-diacetylhexane-2,5-dione along [100]

1.1.3 Theoretical Investigations

DFT calculations were carried out using molecular orbitals theory with GAUSSIAN98 and plane waves theory with periodic boundary conditions using CPMD. After preliminary comparison of different basis sets 6-311++g(d,p) with B3LYP for electron exchange correlation was used for calculations with GAUSSIAN98. David Vanderbilt Ultra Soft Pseudopotentials were used with PBE as functional for density functional theory in CPMD calculations. In all calculations the molecular structure was optimized and the total energy of the three different tautomers (diketo, keto-enole and dienole) of the molecule were calculated. The total energies reveal that the diketo and the mixed keto-enol conformation are far less stable than the dienole. The exact values for total energy and ΔE are summarized in table 1.1. According to the Maxwell-Boltzmann distribution

$$\frac{N_i}{N} = e^{-\frac{\Delta E}{kT}} \tag{1.1}$$

the expected ratio of the different conformations could be calculated. This calculation provides that the diketo and the keto-enol tautomers are only present in extremely low concentrations. For the diketone the concentration is less than 10^{-11}. This is in good agreement to the experimental values, which show neither for ^{1}H and ^{13}C NMR nor for IR spectroscopy a significant signal for carbonyl functionalities. The different tautomers were also

Table 1.1: Total energies for 3,4-diacetylhexane-2,5-dione (GAUSSIAN98)

Conformation	Total energy[H]	ΔE $[kJ \cdot mol^{-1}]$	Ratio
enol	-690.4549	0.00	1.0
keto-enol	-690.4370	46.996	$1.03 \cdot 10^{-9}$
keto	-690.4325	58.811	$5.68 \cdot 10^{-12}$

investigated with CPMD for comparison to the results obtained with GAUSSIAN98. These calculations also showed that the enole conformation is far more stable than the keto form (table 1.2). The calculated ratio between

diketo and dienole is even higher than the one calculated with GAUSSIAN98 and is predicted with $1{:}1.5{\cdot}10^{-18}$. Unfortunately it is not possible to prove the accuracy of these calculated results by experiments because it would exceed analytical possibilities, but in both cases it seems to be a good approximation.

Table 1.2: Total energies for 3,4-diacetylhexane-2,5-dione (CPMD)

Conformation	Total energy[H]	ΔE $[kJ \cdot mol^{-1}]$	Ratio
enol	-129.2116	0.00	1.0
keto-enol	-129.1872	64.062	$5.61{\cdot}10^{-13}$
keto	-129.1761	93.206	$1.50{\cdot}10^{-18}$

Furthermore IR and NMR gradients for all conformations were calculated with GAUSSIAN98 and the diketo and dienole conformation with CPMD. The calculated values of the energetically most stable tautomers were compared to the experimental observed results. GAUSSIAN98 provided very high accuracy between calculated and experimental data for the NMR studies. The differences in the isotropic magnetic shifts were less than 5 % for ^{13}C and less than 0.5 % for ^{1}H NMR signals. In the case of CPMD the results were less accurate, which can be traced back to the fact that the calculation of magnetic shifts is not fully implemented in the program package yet. Therefore the use of David Vanderbilt pseudopotentials, which describe especially transition metals in a better way, was not possible and for the prediction of the magnetic shielding tensor Goedeckers norm conserving pseudo potentials had to be used. Although the results are less exact, they still show the correct trend and therefore allow a comparison between calculated and measured results. In this case the differences in the isotropic magnetic shifts were 18 % for ^{1}H NMR and 28 % for ^{13}C NMR signals (table 1.6 and 1.7).

IR spectroscopy showed for both methods a high quality of the calculations. GUASSIAN98 predicts a vibration at 1652 cm^{-1} for the C=O stretching, which can not be found in the experimental observations. This effect is probably caused by the fast exchange of the proton between the two oxy-

gens. Applying CPMD the carbonyl stretching was not predicted and the measured value of the O-H bending at 1403 cm^{-1} was not obtained. Obviously the cycle formed by enolization is more stable interpreted in CPMD than in GAUSSIAN98, which leads to the right effect for the weakened double bond between carbon and oxygen but inhibits the prediction of the O-H bending.

The shape of the highest occupied molecular orbital (HOMO) and the lowest unoccupied molecular orbitals (LUMO) were calculated with GAUSSIAN98 to identify the character of these orbitals and their possibilities of interaction. The 3D surfaces of the respective orbitals are shown in figure 1.4 and 1.5. The molecular orbital at the oxygen atoms shows for the HOMO and for the LUMO p_x symmetry (defining the C(3)-C(3A) bond as x-axis). The symmetry of the HOMO allows a good interaction with metals consisting of empty *d*-orbitals. Furthermore the HOMO shows a conjugation along the C(2)-C(3)-C(4) bonds. Also it can be noticed that the HOMO and the LUMO orbital show a conjugation along the bridging bond C(3)-C(3A). Furthermore the HOMO and the LUMO show antibonding character of the C=O bond.

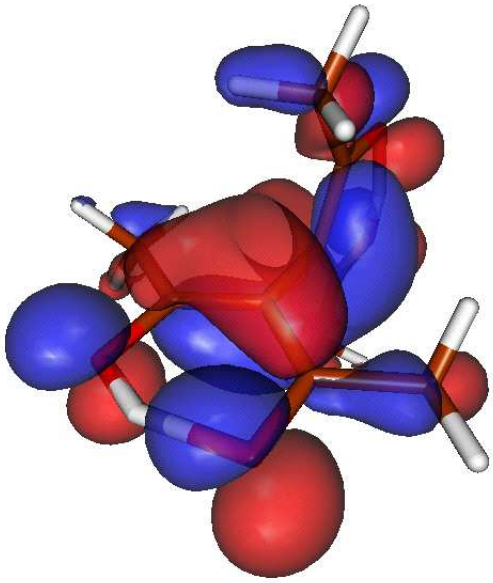

Figure 1.4: HOMO of 2,4-hexane-2,5-dione

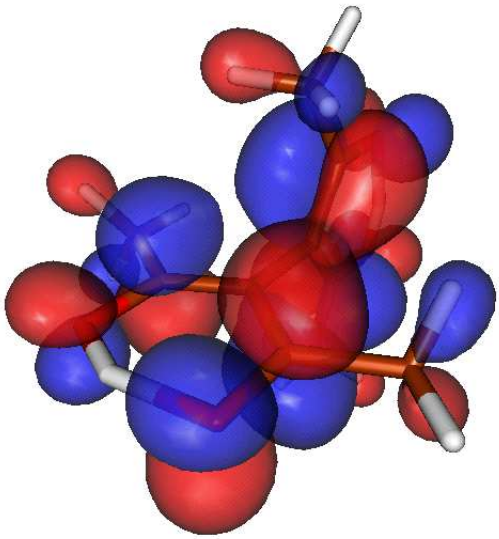

Figure 1.5: LUMO of 2,4-hexane-2,5-dione

Although all calculations are carried out in an ideal environment, i.e. in gaseous phase without any interactions to the surrounding molecules at 0K the comparison to single X-ray diffraction data measured at room temperature in a periodically packed system provides results of high quality. The bond[1] lengths, angles and dihedral angles are shown in table 1.3, 1.4 and 1.5.

Table 1.3: Bond lengths of 3,4-diacetylhexane-2,5-dione

	Bond Length (Å)		
Bond	experimental	GAUSSIAN98	CPMD
O(1)-C(2)	1.3061	1.3241	1.3230
C(1)-C(2)	1.4928	1.5126	1.4972
O(2)-C(4)	1.2755	1.2570	1.2819
C(2)-C(3)	1.3981	1.3897	1.4060
C(3)-C(3A)	1.4942	1.4955	1.4910
C(4)-C(5)	1.4944	1.5126	1.5066

[1]For atom labels see ORTEP plot in Fig. 1.2 on page 21.

Table 1.4: Bond angles of 3,4-diacetylhexane-2,5-dione

	Bond Angle (°)		
Bond	experimental	GAUSSIAN98	CPMD
O(1)-C(2)-C(3)	121.63	121.88	121.98
O(1)-C(2)-C(1)	114.86	112.87	114.54
C(3)-C(2)-C(1)	123.51	125.25	124.48
C(2)-C(3)-C(4)	117.88	117.84	117.07
C(2)-C(3)-C(3A)	121.49	121.64	122.08
C(4)-C(3)-C(3A)	120.63	120.52	120.85
O(2)-C(4)-C(3)	121.39	121.59	121.25
O(2)-C(4)-C(5)	117.39	118.19	117.81
C(3)-C(4)-C(5)	121.21	120.21	120.94

Table 1.5: Torsion angles of 3,4-diacetylhexane-2,5-dione

	Torsion Angle (°)		
Bond	experimental	GAUSSIAN98	CPMD
O(1)-C(2)-C(3)-C(4)	-3.34	0.10	0.44
C(1)-C(2)-C(3)-C(4)	176.29	179.78	179.38
O(1)-C(2)-C(3)-C(3A)	177.12	-179.53	-179.08
C(1)-C(2)-C(3)-C(3A)	-3.24	0.79	1.09
C(2)-C(3)-C(4)-O(2)	2.96	0.11	0.62
C(3A)-C(3)-C(4)-O(2)	-177.50	179.55	-179.85
C(2)-C(3)-C(4)-C(5)	-175.78	179.38	-179.84
C(3A)-C(3)-C(4)-C(5)	3.76	-1.18	-0.31

Table 1.6: ^{1}H NMR data of 3,4-diacetylhexane-2,5-dione

	experimental		GAUSSIAN98		CPMD	
Atom	δ	$\int$	δ	$\int$	δ	$\int$
-CH_3	2.0	12.0	2.0	12.0	1.9	12.0
-OH	16.8	1.8	16.9	2.0	19.8	2.0

Table 1.7: ^{13}C NMR data of 3,4-diacetylhexane-2,5-dione

	experimental	GAUSSIAN98	CPMD
Atom	δ	δ	δ
-CH_3	23.6	25.5	22.7
C(3), C(10)	108.1	107.4	84.5
C=O	192.7	186.5	160.0

Table 1.8: Comparison of IR data

	experimental		GAUSSIAN98		CPMD
Vibration	ν $[cm^{-1}]$	Int.	ν $[cm^{-1}]$	Int.	ν $[cm^{-1}]$
lattice	668	w	648	w	659
lattice	679	w	664	w	684
lattice	913	s	926	w	915
-CH_3 (bend)	997	s	1010	w	997
-CH_3 (bend)	1015	s	1015	w	1011
O-H (bend)	1255	s	1274	m	1145
O-H (bend)	1365	s	1339	s	/
C-H (bend)	1403	s	1402	m	1403
O-H (bend)	1576	s	1636	s	1604
C=O (stretch)	/	/	1652	s	/
O-H (stretch)	3005	w	2792	s	2992

1.2 2,3-Dibenzoyl-1,4-diphenylbutane-1,4-dione

This compound was synthesized to investigate the energetical and sterical effects of the side aromatic substituents at the carbonyl groups and furthermore to prove that ethane-1,1,2,2-tetracarbaldehyde could be used as a model compound for theoretical investigations.

1.2.1 Synthesis

2,3-Dibenzoyl-1,4-diphenylbutane-1,4-dione *(2)* was synthesized in analogy to 3,4-diacetylhexane-2,5-dione in a two step reaction [25]. First dibenzoylmethane was added to a diethyl ether slurry of sodium hydride to form the sodium salt by deprotonation. Afterwards iodine was added and by radical coupling the dimer was formed. The beige precipitate was recrystallized and the pure product was obtained in 0.5% yield, which was a result of the high purity desired for analytical investigations, otherwise yields up to 11% were obtained. The molecular structure of the resulting compound was already described in literature [29] and will be compared to theoretical results.

1.2.2 Characterization

NMR-Spectroscopy

^{1}H NMR spectroscopy in $CDCl_3$ shows a singlet at 6.8 *ppm* for the hydrogens bonded to the C(1) and C(1A) atoms[2], a multiplet in the range of 7.2 - 8.1 *ppm* for the phenyl protons and a singlet at 16.9 *ppm* for the O-H group. This indicates that the obtained structure is present in both tautomer conformations when solved in $CDCl_3$, which is in agreement with the results reported in literature [29] where the signal of the CH group is found at 6.73 *ppm* in $CDCl_3$, however literature did not report signals for the O-H group. ^{13}C NMR spectroscopy in $CDCl_3$ confirms the observation obtained from ^{1}H NMR spectroscopy showing signals at 93.2 *ppm* for C(1) and C(1A), 127.2 - 129.0 *ppm* for the phenyl carbon atoms, 132.5 for C-O, 135.6 for C=O and

[2]For atom labels see ORTEP plot figure 1.6 on page 32.

185.8 for C-O.

IR-Spectroscopy

ATR-FT-IR spectroscopy of the sample shows carbonyl functionalities at 1685 cm^{-1} besides lattice and hydrogen vibrations. The presence of an enolized structure in solid state cannot be proven due to the absence of absorbance bonds typical for enol functionalities. In literature IR spectroscopy was not applied for characterization.

Single Crystal X-Ray Diffraction Analysis

Due to the fact that 2,3-dibenzoyl-1,4-diphenylbutane-1,4-dione is an already known structure crystallographic data were obtained by literature [29]. An ORTEP plot of the structure is shown in figure 1.6. The molecule is present in the diketo form and shows an obvious inversion center in the middle of the C(1)-C(1A) bond. The β-dicarbonyl groups are in cis position and in trans position to the opposite β-dicarbonyl groups. Every two of the opposite phenyls lie in parallel planes. Furthermore all planes spaned by the phenyls are parallel to the direction of the hydrogens bonded to C(1) and C(1A). The length of the C(1)-C(1A) bond is 1.520Å which is insignificantly longer than the equivalent bond for *(1)* with 1.494Å.

1.2.3 Theoretical Investigations

The size of the system did not allow calculations with GUASSIAN98 in reasonable time. The use of smaller basis sets or the combination of different basis sets did not show the necessary accuracy of the results. Therefore calculations were carried out with CPMD to obtain information about the chemical structure and the total energy of the diketo and the enole tautomers. This molecule shows an extreme difference in energy of 270.17 $kJ \cdot mol^{-1}$ for the two tautomers (table 1.9). According to this result the expected ratio of the enol isomer is below 10^{-51}, which indicates that it is not stable in solid state.

Table 1.9: Total energy, energy differences and expected ratio

Conformation	Total energy[H]	ΔE $[kJ \cdot mol^{-1}]$	Ratio
keto	-247.6085	0.00	1.0
enol	-247.5056	270.165	$2.18 \cdot 10^{-52}$

As a model compound for this structure ethane-1,1,2,2-tetracarbaldehyde *(2A)* was calculated with GAUSSIAN98, which was expected as a usable simplification [30]. However, further calculations and structure analysis showed that it is not an appropriate model, due to the steric demand of the phenyls that influences the molecular structure significantly. Also for *(2A)* the HOMO and LUMO were calculated and show the same characteristics as 2,4-diacetylhexane-2,5-dione at the oxygens (figure 1.7 and 1.8). This allows the assumption, that the nature of the substituent in α position has a negligible effect to the electronic configuration at the point where coordination occurs. Also can be noticed that this simplification would predict that the dienole confor-

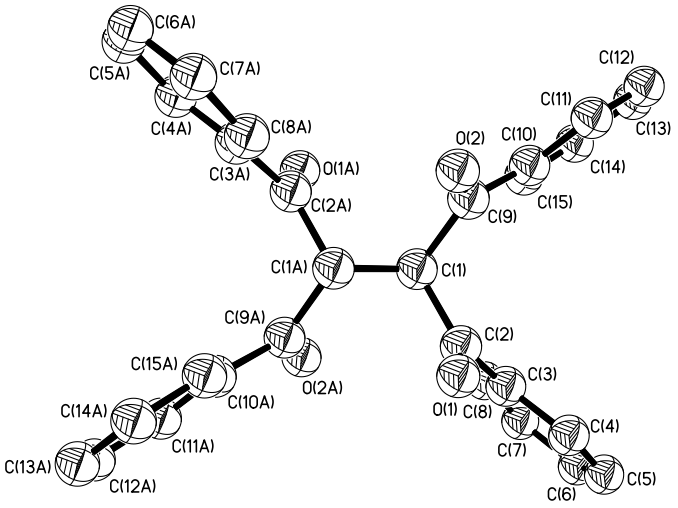

Figure 1.6: ORTEP plot of 2,3-dibenzoyl-1,4-diphenylbutane-1,4-dione

mation is more stable which is in disagreement to X-ray structure analysis and calculations of the whole molecule.

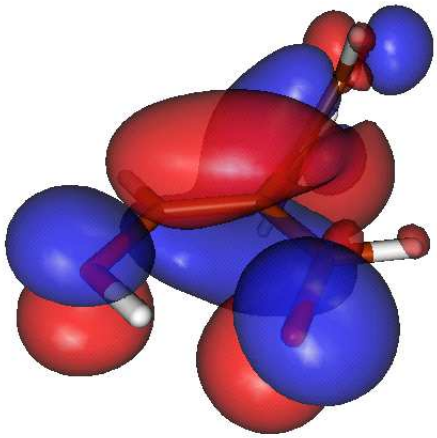

Figure 1.7: HOMO of 1,1,2,2-tetracarbaldehyde

Structure optimization and vibrational analysis showed a very high accuracy to X-ray structure which is present in the diketo form. The obtained results for bond lengths (table 1.10), bond angles (table 1.11) and torsion angles (table 1.12) are in very good agreement between theory and experimental results. The lengths of the carbon-carbon bonds are in the range of 1.52 to 1.54 Å near to the carbonyls. Also the carbonyls show no significant difference in length, which also indicates that a stable 1,3-dicarbonyl is obtained. Again a systematic elongation of the bond angles can be noticed.

Table 1.10: Bond lengths of 2,3-dibenzoyl-1,4-diphenylbutane-1,4-dione

	Bond Length (Å)	
Bond	experimental	CPMD
C(9)-C(10)	1.4813	1.4942
C(9)-O(2)	1.2190	1.2319
C(9)-C(1)	1.5407	1.5478
C(1)-C(2)	1.5209	1.4930
C(2)-O(1)	1.2203	1.2322
C(2)-C(3)	1.4794	1.4942
C(1)-C(1A)	1.5198	1.5326

Table 1.11: Bond angles of 2,3-dibenzoyl-1,4-diphenylbutane-1,4-dione

	Bond Angle (°)	
Bond	experimental	CPMD
C(10)-C(9)-C(1)	120.73	119.05
C(9)-C(1)-C(2)	107.17	106.67
C(1)-C(2)-C(3)	121.86	119.27
C(10)-C(9)-O(2)	121.23	121.24
O(2)-C(9)-C(1)	118.01	119.66
C(1)-C(2)-O(1)	118.45	119.82
O(1)-C(2)-C(3)	119.69	120.85

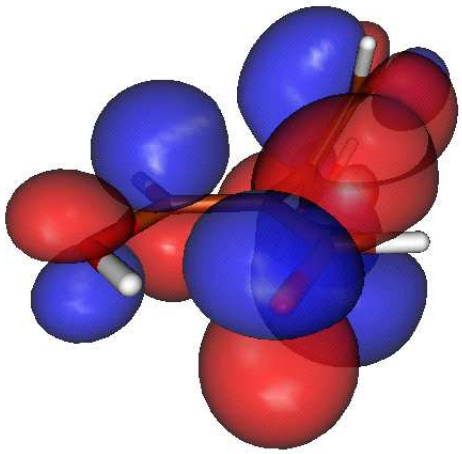

Figure 1.8: LUMO of 1,1,2,2-tetracarbaldehyde

Table 1.12: Torsion angles of 2,3-dibenzoyl-1,4-diphenylbutane-1,4-dione

	Torsion Angle (°)	
Bond	experimental	CPMD
C(10)-C(9)-C(1)-C(2)	87.97	86.06
C(9)-C(1)-C(2)-C(3)	-101.04	-98.10
O(2)-C(9)-C(1)-C(2)	-89.99	-91.12
C(9)-C(1)-C(2)-O(1)	78.55	79.37
C(9)-C(1)-C(1A)-C(2A)	180.00	178.90
C(9)-C(1)-C(1A)-C(9A)	61.76	63.14

Isotropic magnetic shifts were calculated for ^{1}H and ^{13}C NMR and compared to the experimental values in relation to TMS. The results for ^{1}H NMR spectroscopy showed a good correlation for the phenyls in the range of 7.2 to 8.1 *ppm*, while the result for the protons at position C(3) and C(3A), which is predicted with 8.0 *ppm*, is far to high. The experimental value for this hydrogen is 6.8 *ppm*. Due to the calculation of the more stable keto tautomer no values of the hydroxy group was provided, which was experimentally obtained at 16.9 *ppm*. The shifts obtained for ^{13}C NMR show no significance, because of differences up to 52%. Even the trend is not given in this calculation.

Table 1.13: ^{1}H NMR data of 2,3-dibenzoyl-1,4-diphenylbutane-1,4-dione ($CDCl_3$)

	experimental		calc.
Atom	δ	$\int$	δ
C-H	6.8	1.1	8.00
ph-H	7.2-7.7	11.7	6.79
ph-H	7.2-7.7	11.7	6.82
ph-H	7.9-8.1	8.0	7.69
O-H	16.9	1.0	n.a.

The data obtained for infrared spectroscopy showed an excellent correlation (table 1.15). The calculation with CPMD allows the interpretation of every peak of the quite complex spectrum. As one example the peak for the carbonyl functionality predicted with 1659 cm^{-1} only deviates from the experimental obtained value by 26 cm^{-1}. This confirms that in solid state only the keto conformation is present.

Table 1.14: ^{13}C NMR data of 2,3-dibenzoyl-1,4-diphenylbutane-1,4-dione ($CDCl_3$)

	experimental	calc.
Atom	δ	δ
ph	127.2	61.25
ph	127.5	62.31
ph	127.9	62.31
ph	128.2	74.24
ph	128.7	74.24
ph	129.0	74.55
C-H	93.2	106.7
C-O	132.5	n.a.
C=O	135.6	116.0
O-H	185.8	n.a.

Table 1.15: IR data of 2,3-dibenzoyl-1,4-diphenylbutane-1,4-dione

	experimental		CPMD
Vibration	ν $[cm^{-1}]$	Int.	ν $[cm^{-1}]$
lattice	668	w	671
lattice	695	w	697
lattice	708	m	716
lattice (phenyl)	861	w	861
lattice (phenyl)	931	w	921
lattice (phenyl)	980	w	982
lattice (phenyl)	1026	w	1022
lattice (phenyl)	1073	w	1077
lattice	1198	w	1180
lattice	1263	w	1269
lattice	1286	m	1288
lattice	1319	m	1320
lattice (phenyl)	1366	s	1390
lattice (phenyl)	1413	s	1421
lattice (phenyl)	1448	s	1468
lattice (phenyl)	1597	m	1591
C=O (stretch)	1685	m	1659
C-H (stretch)	3040	w	3039
C-H (stretch,phenyl)	3060	w	3065

1.3 Tetramethyletane-1,1,2,2-tetracarboxylate

This dimer diether compound was synthesized for comparison to the other β-diketones by exchanging the keto with carboxy late ester groups. The ester groups are more flexible than the phenyl groups therefore another steric demand is given. Furthermore the carboxy ester should show a different behavior according to the effect of enolization and also the electronical properties are different which should result in a modification of coordination.

1.3.1 Synthesis

This compound was synthesized in analogy to the other molecules discussed before. It was prepared by dropwise addition of dimethylmalonate to a well diluted diethyl ether slurry of sodium hydride. After the sodium salt was prepared iodine was added under reflux which resulted in the formation of tetramethyletane-1,1,2,2-tetracarboxylate *(3)* by radical coupling as a white solid in 53% yield.

1.3.2 Characterization

NMR-Spectroscopy

^{1}H NMR spectroscopy showed singlets at 3.8 *ppm* for the mehtyl groups and at 4.2 *ppm* for the hydrogens bonded to the atoms[3] C(2) and C(2A). This indicates that the expected carboxy functionality is present and no tautomerism forming an enolized structure occurred. This is also confirmed by ^{13}C NMR spectroscopy. The spectrum shows signals at 51.1 *ppm*, 53.2 *ppm* and 167.5 *ppm* for the methyl groups, the bridging carbonyls and the carbonyls of the ester. Table 1.16 and 1.17 show the summarized results for ^{1}H and ^{13}C NMR spectroscopy.

[3]For atom labels see ORTEP plot figure 1.9 on page 42

Table 1.16: ^{1}H NMR data of tetramethyletane-1,1,2,2-tetracarboxylate ($CDCl_3$)

	experimental		calculated	
Atom	δ	$\int$	δ	$\int$
-CH_3	3.8	12.0	4.0	12.0
-CH	4.2	2.0	4.4	2.0

Table 1.17: ^{13}C NMR data of tetramethyletane-1,1,2,2-tetracarboxylate

	experimental	calculated
Atom	δ	δ
CH	51.1	39.1
CH_3	53.2	49.4
COO	167.5	138.6

IR-Spectroscopy

Similar to 2,3-dibenzoyl-1,4-diphenylbutane-1,4-dione the vibrational spectrum of tetramethyletane-1,1,2,2-tetracarboxylate shows beside vibrations of the lattice and hydrogens only carbonyls at 1716 cm^{-1} and 1741 cm^{-1} (table 1.18). This indicates that in solution and in solid state only carboxy ester groups are present. 2,3-diacetylhexane-2,5-dione which is, according to the functionalities more similar to this structure, could only be found as dienole forming a stable six membered cycle. This enolization with a concomitant delocalization of the electrons is obviously inhibited by the carboxy late functionality.

Table 1.18: IR data of tetramethyletane-1,1,2,2-tetracarboxylate

	experimental		CPMD
Vibration	ν $[cm^{-1}]$	Int.	ν $[cm^{-1}]$
lattice	888	m	786
lattice	997	s	983
lattice	1154	s	1083
lattice	1174	s	1109
lattice (C(2)-C(2A))	1192	m	1189
lattice	1270	s	1289
lattice	1311	s	1298
lattice	1440	s	1360
C=O (stretch)	1716	s	1858
C=O (stretch)	1741	s	1885
C-H (stretch)	???	?	4300
C-H (stretch)	???	?	4500

X-Ray Diffraction

The obtained powder was recrystallized in acetonitrile forming suitable crystals for single crystal X-ray diffraction studies. An ORTEP plot of the ob-

tained molecule is shown in figure 1.9. As already assumed in NMR and IR spectroscopy the solid is present as a β-diketone. Similar to *(2)* the 1,3-carboxy groups are in cis position and in comparison to the opposite dicarbonyl functionality in trans position. Also an obvious inversion in the center of the C(2)-C(2A) bond is obtained. Any planar structures that would indicate a stabilization of the structure by electron delocalization can not be observed. Also the bond lengths (table 1.19) of the oxygens O(1) and O(2) bonded to the carbon C(1) show a significant difference. The atoms C(1), C(2), O(1) and O(2) show a planar structure resulting from the sp^2 hybridization of C(1). All carbon-carbon bonds (table 1.20 and 1.21) show typical length and geometries of an aliphatic system.

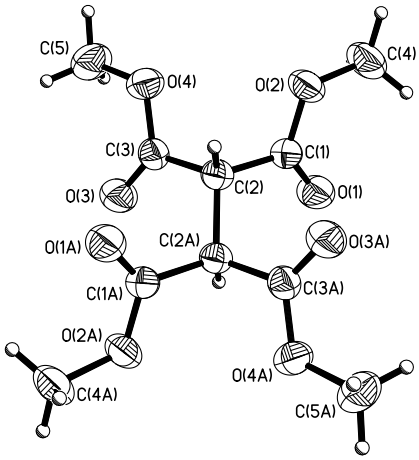

Figure 1.9: ORTEP plot of tetramethyletane-1,1,2,2-tetracarboxylate

Figure 1.10 shows the crystal packing of the obtained molecule along the [100] axis. Even though the structure contains quite acid hydrogens a stabilization of the molecular structure by forming interatomic hydrogen bridges can not be observed.

Table 1.19: Experimental and calculated bond lengths of tetramethyletane-1,1,2,2-tetracarboxylate

	Bond Length (Å)	
Bond	experimental	CPMD
O(1)-C(1)	1.1958	1.2224
C(1)-O(2)	1.3205	1.3588
C(1)-C(2)	1.5235	1.5310
O(2)-C(4)	1.4463	1.4579
C(2)-C(3)	1.5233	1.5338
C(2)-C(2A)	1.5276	1.5326
O(3)-C(3)	1.1932	1.2214
C(3)-O(4)	1.3233	1.3602
O(4)-C(5)	1.4497	1.4560

Table 1.20: Experimental and calculated bond angles of tetramethyletane-1,1,2,2-tetracarboxylate

	Bond Angle (°)	
Bond	experimental	CPMD
O(1)-C(1)-O(2)	124.87	124.60
O(1)-C(1)-C(2)	123.80	124.01
O(2)-C(1)-C(2)	111.33	111.37
C(1)-O(2)-C(4)	116.61	113.67
C(3)-C(2)-C(1)	108.93	108.97
C(3)-C(3)-C(2A)	110.04	109.75
C(1)-C(2)-C(2A)	110.81	109.79
O(3)-C(3)-O(4)	124.53	124.46
O(3)-C(3)-C(2)	124.08	124.49
O(4)-C(3)-C(2)	111.39	111.05
C(3)-O(4)-C(5)	115.64	114.18

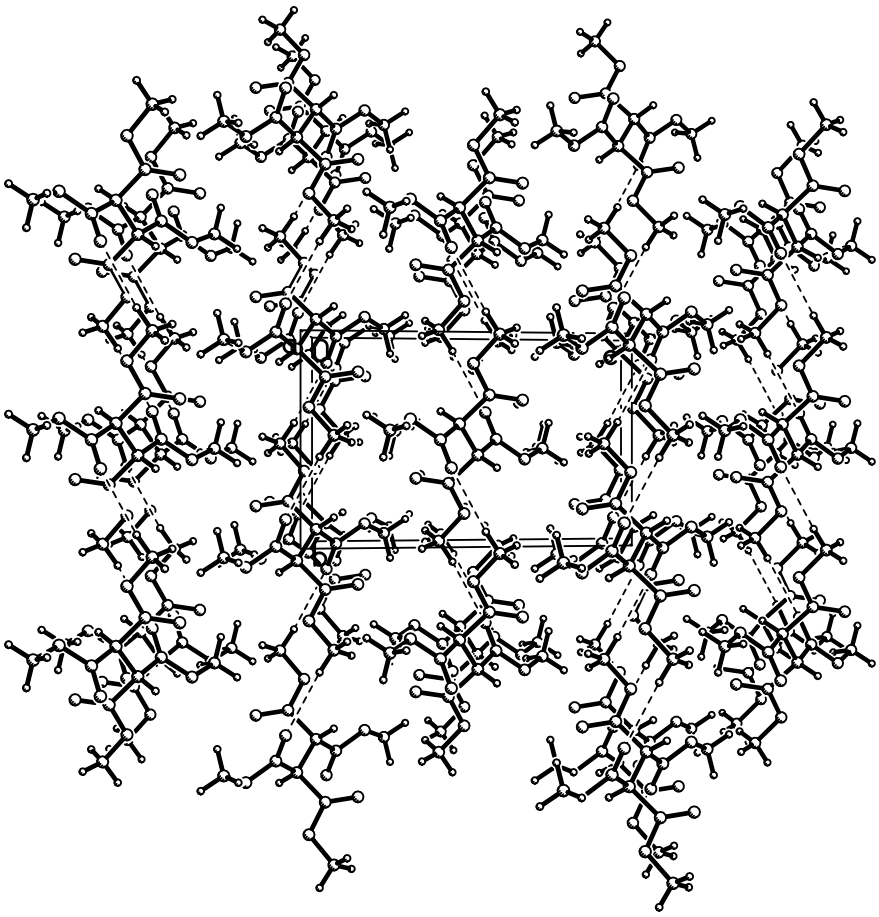

Figure 1.10: Crystal packing along [100] axis of tetramethyletane-1,1,2,2-tetracarboxylate

1.3.3 Theoretical Investigations

This system was also geometry optimized and investigated with CPMD. In comparison to the already discussed systems the obtained results are of less accuracy. The most obvious reason for this observation is a not well optimized pseudopotential for oxygen and the high amount of oxygen atoms, which are also a part of the lattice. The theoretical results are still exact enough to allow a good interpretation of the spectra.

Compared to the data obtained from the crystal structure analysis the obtained optimized structure shows negligible differences and are summarized in table 1.19, 1.20 and 1.21. Again in this system the systematical elongation of the bond lengths can be found, which is up to 2% for the carbonyls and 1% for the other bonds. The prediction of the isotropic magnetical shifts for ^{1}H NMR spectroscopy shows an adequate accuracy to the experimental values. The difference between the shifts for the methyl groups as for the hydrogen of the bridging carbons[4] C(2) and C(2A) is in both cases 0.2 *ppm*. Computationally obtained shifts for ^{13}C NMR show a low accuracy with differences to the experimental values up to 28.9 *ppm* but the trend is still given. The derived results of vibrational analysis are far less accurate then obtained for 3,4-diacteylhexane-2,5-dione and 2,3-dibenzoyl-1,4-diphenylbutane-1,4-dione. As mentioned the most obvious reason for this observation is an inaccurate pseudopotential for oxygen and the high number of oxygens. As table 1.18 shows the difference between calculated and experimental wave numbers is mainly in the range of $100cm^{-1}$ and goes up to $144cm^{-1}$ for the carbonyl groups. However, the results are still interpretable and the absorbance bands attributable.

[4]For labels see the ORTEP plot of the determined structure (figure 1.9).

Table 1.21: Experimental and calculated torsion angles of Tetramethyletane-1,1,2,2-tetracarboxylate

	Torsion Angle (°)	
Bond	experimental	CPMD
C(1)-C(2)-C(3)-C(4)	87.97	86.06
C(2)-C(3)-C(4)-C(5)	-101.04	-98.10
O(1)-C(2)-C(3)-C(4)	-89.99	-91.12
C(2)-C(3)-C(4)-O(2)	78.55	79.37
C(2)-C(3)-C(3A)-C(2A)	180.00	178.90
C(2)-C(3)-C(3A)-C(4A)	61.76	63.14

Table 1.22: Total energy, energy differences and expected ratio

Conformation	Total energy[H]	ΔE $[kJ \cdot mol^{-1}]$	Ratio
keto	-193.1979	0.00	1.0
enol	-187.9289	13 833.833	0.0

Chapter 2

Metal-Ligand-Systems

This chapter discusses the different attempts carried out to obtain structured networks formed by the reaction of 3,4-diacetylhexane-2,5-dione with different metal ions. In order to obtain uncharged systems for each ligand, that coordinates, one positive charge must be present at the ion. Two different forms of structured systems can be obtained. For metal ions of the charge 2+ two ligands coordinate to the metal center forming linear structures. This system was investigated with copper(II) salts, where a square-planar coordination is expected [31, 32, 33, 34, 35]. For charges of 3+ and higher 3D structures are formed. For the systems, which are formed by metal(III) salts an octahedral coordination should be found. Two systems could be investigated formed by aluminium and yttrium as coordination centers. For all syntheses the ligand and the salt were separately dissolved in the same solvent and afterwards united forming the coordination structure. Therefore the anions had to be soluble in the appropriate solvent and further had to show less affinity to the ion than the ligand.

2.1 Tris(3,4-diacetylhexane-2,5-dione)aluminium

The reaction of 3,4-diacetylhexane-2,5-dione with an aluminium(III) salt is expected to form a three dimensional network through an octahedral coordination of the aluminium ion by three ligand anions. Aluminium nitrate

was mixed with the sodium salt of 3,4-diacetylhexane-2,5-dione in the ratio of 1:1.5 with ethanol as solvent at room temperature. After one day a colorless precipitate was formed that was characterized by IR spectroscopy, ^{13}C and ^{29}Al MAS NMR spectroscopy and elemental analysis. Single X-ray structure analysis could not be carried out due to no usable crystals were formed. ^{29}Al MAS NMR showed an overlap of two wide peaks at -5.0 ppm indicating an octahedral coordination of aluminium by two different ligands. This allows the interpretation that a partial reaction between ligand and metal took place. ^{13}C MAS NMR indicates also a reaction of the ligand by additional peaks at 12.2 and 55.7 ppm and a shift of the carbonyl carbon signals from 192.7 ppm to 179.2 ppm. Neither an interpretation how the ligand coordinated nor to determine the amount of conversion were possible. The assumption of an only partial reaction is also supported by elemental analysis which showed a fifth of the theoretical carbon content provided by a full substitution and 7.8% nitrogen resulting from remaining nitrate. The IR spectrum of the solid showed a total conversion of the ligand by elimination of all absorption bands of enol OH-groups at 1255 to 3005 cm^{-1} present in the free ligand. Variations of the reaction conditions by varying ligand metal ratio, temperature, solvent and pressure did not lead to precipitates providing better results. In the most cases no precipitate was formed or only colloide systems were obtained.

The experimental results were compared to DFT calculations carried out using CPMD on a model structure (figure 2.1) containing the bridging ligand with two aluminium atoms coordinated to it, the additional coordination sites at the Al-atoms were saturated with pentane-2,5-dione. For calculations no simplifications were applied that would assume a symmetry of the obtained structure, therefore the applied space group was C_1. The geometry of the structure was optimized and a vibrational analysis was carried out. The six membered ring formed by the coordination of the oxygen atoms to the aluminium ion shows nearly the same planarity as found in the calculations of the enolized structure of the ligand. The equivalent bonds show no significant difference in length and the deflection of the cycle reaches a maximum of 6.5 degrees. The vibrations influenced by the bridging ligand were de-

termined and compared to the experimental results. As shown in table 2.1 the computational data are in good agreement with the experimental data showing a maximum error of 12 cm^{-1} for the bending of the methyl groups. According to the comparison of calculated and measured IR data only coordinated ligand could be found. This indicates that the precipitate is formed by the reaction of the bridging ligand with the metal salt but according to elemental analysis the ratio of conversion for the salt is very low. Due to the only partial conversion of the aluminium salt no regular network was formed.

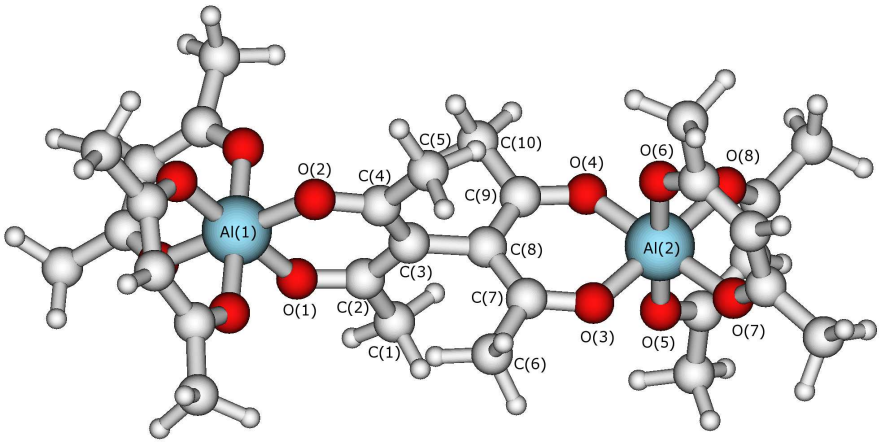

Figure 2.1: Model aluminium structure used for calculations

Table 2.1: Calculated data of the aluminium-ligand structure

Bond Length (Å)		Bond Angles (°)		Dihedral Angle (°)	
Bond	calc.	Atoms	calc.	Atoms	calc.
Al(1)-O(1)	1.8986	O(1)-Al(1)-O(2)	89.94	C(2)-C(3)-C(8)-C(9)	88.82
Al(1)-O(2)	1.8945	Al(1)-O(1)-C(2)	129.94	Al(1)-O(1)-C(2)-C(3)	3.95
O(1)-C(2)	1.2892	Al(1)-O(2)-C(4)	130.06	Al(1)-O(2)-C(4)-C(3)	-4.71
O(2)-C(4)	1.2901	C(2)-C(3)-C(4)	120.15	C(8)-C(7)-O(3)-Al(2)	1.05
C(1)-C(2)	1.5105	C(1)-C(2)-C(3)	120.11	C(8)-C(9)-O(4)-Al(2)	-6.47
C(2)-C(3)	1.4230	C(3)-C(4)-C(5)	120.53		
C(3)-C(4)	1.4219	C(2)-C(3)-C(8)	120.02		
C(4)-C(5)	1.5106	C(4)-C(3)-C(8)	119.80		
C(3)-C(8)	1.4998	C(3)-C(8)-C(7)	120.73		
C(6)-C(7)	1.5099	C(3)-C(8)-C(9)	119.27		
C(7)-C(8)	1.4215	C(7)-C(8)-C(9)	120.00		
C(8)-C(9)	1.4247	C(6)-C(7)-C(8)	121.30		
C(9)-C(10)	1.5104	C(8)-C(9)-C(10)	120.12		
C(7)-O(3)	1.2907	C(7)-O(3)-Al(2)	130.39		
C(9)-O(4)	1.2887	C(9)-O(4)-Al(2)	129.93		
O(3)-Al(2)	1.8927	O(3)-Al(2)-O(4)	89.88		
O(4)-Al(2)	1.8961	O(3)-Al(2)-O(5)	89.32		
Al(2)-O(5)	1.9003	O(4)-Al(2)-O(5)	91.94		
Al(2)-O(6)	1.9075	O(3)-Al(2)-O(7)	90.02		
Al(2)-O(7)	1.9146	O(3)-Al(2)-O(8)	179.13		
Al(2)-O(8)					

2.2 Tris(3,4-diacetylhexane-2,5-dione)yttrium

Another investigated coordination compound was tris(3,4-diacetylhexane-2,5-dione)yttrium. The coordination product was synthesized by reaction of 3,4-diacetylhexane-2,5-dione with yttrium nitrate in the ratio of 1:1.5. To obtain the best results for the precipitate the two solids were solved in acetonitrile and the solutions united afterwards. A few hours later colorless crystals were formed but single crystal X-ray diffraction showed that only the ligand had precipitated. To obtain coordination between metal and ligand the solution was filtered and put under a triethyl-ammonia saturated atmosphere to achieve coordination by deprotonation of the ligand [1], which results in a higher concentration of yttrium nitrate than in the initial mixture. After a few days a gel was formed that was dried in vacuo and investigated using IR spectroscopy. According to the small amount of the formed solid no elemental analysis could be carried out. Also in this case this procedure showed the best results for a series of preparation attempts carried out by variating metal to ligand ratio, temperature, pressure and solvent.

The results were also compared to theoretical results achieved by DFT calculations using a model structure containing the dianionic ligand coordination to two yttrium ions, which are saturated with acetylacetone similar

Table 2.2: Comparison of experimental and calculated IR data for the aluminium complex

	experimental		CPMD
Vibration	ν $[cm^{-1}]$	Int.	ν $[cm^{-1}]$
Al-O (stretch)	676	m	681
bridging C-C (sym.)	948	m	944
-CH_3 (bend)	1049	m	1037
bridging C-C (asym.)	1355	s	1351
CO-C-CO (stretch)	1469	s	1466
C=O (stretch)	1581	s	1579

to the Al-compound. The structure was geometry optimized (figure 2.2) and vibrational analysis was carried out. Although the obtained results are less

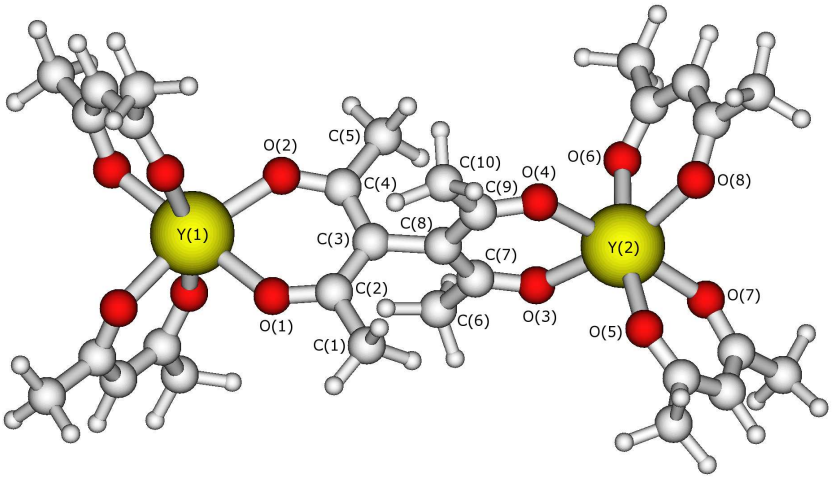

Figure 2.2: Model yttrium complex used for calculations

accurate than those achieved for the aluminium system they allow an interpretation of the reaction. The different accuracy provided in the calculations are a result of the used ultra soft pseudopotentials [36]. The obtained potentials were mainly optimized for the characterization of ionic crystal structures and only adapted to the applied exchange correlation method, which results in incidentally problems for the convergence of the wavefunction during geometry optimizations. Whereas the resulting error was quite negligible for

aluminium it showed noticeable effects for yttrium. This results in differences for obvious equivalent bond lengths as shown in table 2.4. The obtained dihedral angels show less planarity of the by coordination formed cycle with a deflection up to 24.6 degrees. The comparison of experimental and calculated IR absorption bands is summarized in table 2.3. Similar to the aluminium complex the resulting bands support a coordination of the dianionic structure to the metal. A crystalline structure usable for single X-ray structure analysis was not obtained.

2.3 Bis(3,4-diacetylhexane-2,5-dione)copper

Investigations on copper(II) salts were carried out to achieve information about the usability of the ligand to form linear structures. According to the charge of the copper ion only two bridging ligands can coordinate. Therefore a regular and linear structure is expected. The attempt to obtain linear structures with copper resulted in analogy to the previously discussed systems in non crystalline precipitates. In this case the copper ions are expected to form a square-planar structure with the chelating ligands [31, 32, 33, 34, 35]. According to IR spectroscopy a partial reaction took place. The possibility that the low conversion is the result of a formed side product could not be

Table 2.3: Comparison of experimental and calculated IR data for the yttrium complex

	experimental		CPMD
Vibration	$\nu\ [cm^{-1}]$	Int.	$\nu\ [cm^{-1}]$
lattice	689	w	698
bridging C-C (asym.)	1161	w	1198
C-CH_3 (stretch)	1306	s	1304
C=O (stretch, asym.)	1361	s	1359
C=O (stretch, sym.)	1575	m	1553
CH_3 (stretch)	2990	w	2968

Table 2.4: Calculated data of the yttrium-ligand structure

Bond Length (Å)		Bond Angles (°)		Dihedral Angle (°)	
Bond	calc.	Atoms	calc.	Atoms	calc.
Y(1)-O(1)	2.2867	O(1)-Y(1)-O(2)	78.13	C(2)-C(3)-C(8)-C(9)	-102.18
Y(1)-O(2)	2.2034	Y(1)-O(1)-C(2)	123.00	Y(1)-O(1)-C(2)-C(3)	-7.75
O(1)-C(2)	1.2871	Y(1)-O(2)-C(4)	133.47	Y(1)-O(2)-C(4)-C(3)	-24.56
O(2)-C(4)	1.2900	C(2)-C(3)-C(4)	123.56	C(8)-C(7)-O(3)-Y(2)	-8.64
C(1)-C(2)	1.5140	C(2)-C(3)-C(8)	120.91	C(8)-C(9)-O(4)-Y(2)	-25.85
C(2)-C(3)	1.4321	C(4)-C(3)-C(8)	115.47		
C(3)-C(4)	1.4208	C(3)-C(8)-C(7)	117.78		
C(4)-C(5)	1.5151	C(3)-C(8)-C(9)	117.91		
C(3)-C(8)	1.4975	C(7)-C(8)-C(9)	123.52		
C(6)-C(7)	1.5124	C(6)-C(7)-C(8)	120.95		
C(7)-C(8)	1.4287	C(8)-C(9)-C(10)	120.80		
C(8)-C(9)	1.4300	C(7)-O(3)-Y(2)	132.38		
C(9)-C(10)	1.5134	C(9)-O(4)-Y(2)	129.93		
C(7)-O(3)	1.2903	O(3)-Y(2)-O(4)	79.75		
C(9)-O(4)	1.2909	O(3)-Y(2)-O(5)	97.52		
O(3)-Y(2)	2.2171	O(4)-Y(2)-O(5)	98.97		
O(4)-Y(2)	2.2206	O(4)-Y(2)-O(6)	88.54		
Y(2)-O(5)	2.2253	O(3)-Y(2)-O(7)	99.76		
Y(2)-O(6)	2.3060	O(3)-Y(2)-O(8)	164.83		
Y(2)-O(7)	2.2807	O(4)-Y(2)-O(7)	178.22		
Y(2)-O(8)	2.2444				

verified by spectroscopical methods. It was not possible to carry out NMR spectroscopy due to the paramagnetic effect of copper. Comparison to DFT calculations failed in this case, because of the adapted pseudopotential that was used for copper[36] did not show convergence for geometry optimization and vibrational analysis for the investigated system. Elemental analysis showed that obtained precipitate contained only 4.6% carbon, which is a great difference to the expected 45.5% carbon, of bis(3,4-diacetylhexane-2,5-dione)copper. This indicates that the desired conversion occurred only in a low ratio.

Chapter 3

Theoretical Investigations on ATRP Initiators

This chapter discusses the electronical characteristics of initiators for atomic transfer radical polymerization. The polymerization is initiated by the homogenous cleavage of a halide carbon bond. The obtained radical adds to a vinyl group containing monomer forming a new radical at the end of the resulting chain. Two kinds of initiators were investigated using *ab initio* calculations to determine the necessary energy of cleavage and electronical properties. The first group are initiators that are commonly applied and well characterized. The other group are novel ligands that show the possibility to coordinate to metal ions and also contain initiating groups. The electronic conformation this work focuses on is the local spin density, which allows a prediction where the reaction between the initiator and the monomer takes place.

3.1 Conventional Initiators

The initiators discussed in this section are commonly applied and already theoretically investigated by *ab initio* calculations [37]: methyl 2-bromopropionate (1), methyl 2-bromo-2-methylpropionate (2) and 1-phenylethyl bromide (3) (figure 3.1). For this initiators and the respective radicals a study was carried

out to determine energetical and electronical properties. Furthermore the obtained data were compared to other theoretical and experimental gained values to prove the accuracy of the method applied in this work. The geometries were optimized and vibrational analysis was carried out using DFT calculations and the local spin densities were determined using limited configuration interaction, which provided results of very high precision [38].

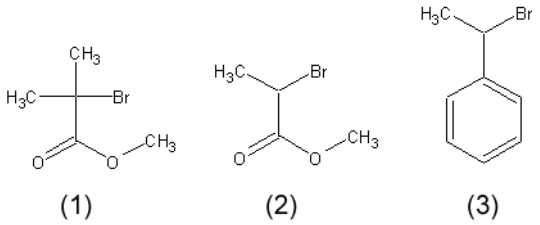

Figure 3.1: Initiators for ATRP

3.1.1 Energy of Cleavage

The structures of the initiators, the corresponding radicals and the halides were optimized and afterwards vibrational analysis was carried out to derive enthalpies, entropies and free energies of the compounds. The bond dissociation energies were determined by calculating the difference of the energies of the initiator and the cleaved parts [37]. The obtained thermochemical values are listed in table 3.1. According to these results *initiator (1)* shows the lowest necessary energy of 215.6 $kJ \cdot mol^{-1}$ for breaking the carbon-halide

Table 3.1: Energy of cleavage for ATRP initiators (DFT)

Initiator	ΔH°_{298} $[kJ \cdot mol^{-1}]$	ΔS°_{298} $[J \cdot mol^{-1}]$	ΔG°_{298} $[kJ \cdot mol^{-1}]$
(1)	262.4	157.0	215.6
(2)	266.6	141.9	224.3
(3)	265.0	140.9	223.0

bond. *Initiator (2)* and *(3)* showed slightly higher dissociation energies of 224.3 $kJ \cdot mol^{-1}$ and 223.0 $kJ \cdot mol^{-1}$, which are very similar, although the molecular structures are quite different. These results were compared to an earlier work [37], where a different basis set and another exchange correlation potential were used (6-31**; B3P86). The reported values are 206.7 $kJ \cdot mol^{-1}$, 216.7 $kJ \cdot mol^{-1}$ and 219.7 $kJ \cdot mol^{-1}$ for the initiators *(1)*, *(2)* and *(3)*, which is an excellent agreement.

3.1.2 Local Spin Densities

For further investigations the local spin densities of the discussed initiators were calculated. All initiators show a high spin density at the place were the cleavage occurred (figure 3.2, 3.3 and 3.4). This is most obvious for *initiator (1)* were most of the spin density is located in position 2 of the carbon chain and shows only negligible densities at the oxygen atom contrary to *initiators (2)* and *(3)*, which do not show such a high localization. *Initiator (2)* also shows a high spin density at the oxygen atom and *(3)* a symmetrical distribution at the phenol ring.

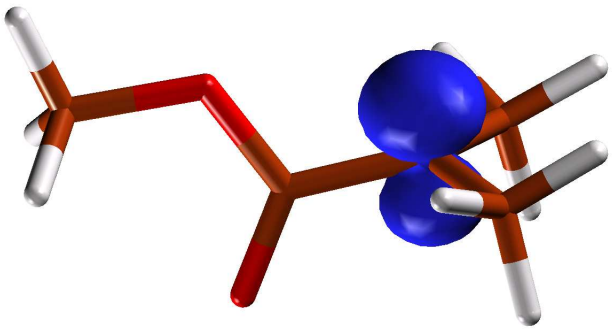

Figure 3.2: Spin density plot of initiator (1)

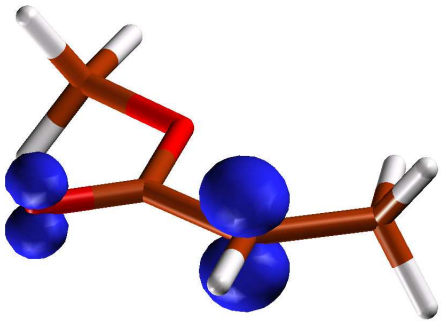

Figure 3.3: Spin density plot of initiator (2)

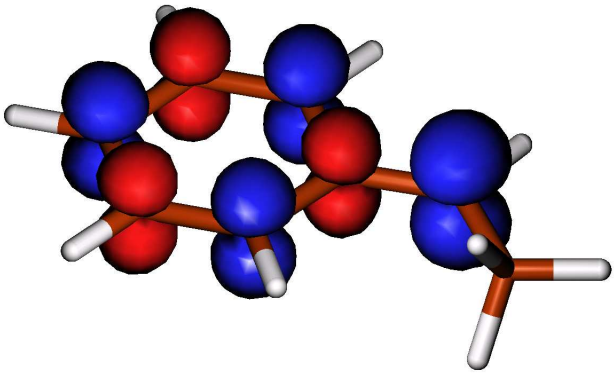

Figure 3.4: Spin density plot of initiator (3)

3.2 β-Diketones as Initiators for ATRP - A Theoretical Study

In this section the energetic and electronical properties of 3-chloro-2,4-pentandione and 3-bromo-2,4-pentandione are discussed. These initiators can act as bidentate ligands that coordinate to metal via the two oxygen atoms after deprotonation. The initiators were calculated in the same way as those described in the chapter before, using DFT for geometry optimization and energetical characterization. Limited configuration interaction was applied for determination of the spin densities.

3.2.1 Energy of cleavage

According to the investigations carried out in the chapter *"Synthesis, Characterization and Theoretical Investigations of β-Diketones"* the diketone and the enolized structures were optimized and vibrational analysis were applied. The calculations derived that for both halide derivates the enolized structures were the more stable, for which the necessary energy for bond dissociation was investigated. The obtained thermochemical values (table 3.2) show that the difference between the necessary energies is less than 1.5% for the two compounds. In comparison to the previous discussed initiators the energy of cleavage is more than 90 $kJ \cdot mol^{-1}$ higher. These calculations neglect the influence of a metal ion to which the initiator will be coordinated. It must be further considered that in case of coordination to a metal ion the displacement of electron density influences the stability of the radical. Therefore

Table 3.2: Energy of cleavage for ATRP initiators (DFT)

Initiator	ΔH°_{298} $[kJ \cdot mol^{-1}]$	ΔS°_{298} $[J \cdot mol^{-1}]$	ΔG°_{298} $[kJ \cdot mol^{-1}]$
3-chloro-2,4-pentandione	366.2	150.9	321.2
3-bromo-2,4-pentandione	365.5	163.7	316.7

it can be expected that the energy shows higher values for cleavage of the coordinated ligand.

3.2.2 Local spin densities

To investigate the behavior of the radical the spin density of the enolized compound was calculated applying limited configuration interaction calculations. A similar planar structure is expected for the coordinated molecule. The obtained spin density is shown in figure 3.5.

By this the starting point for polymerization of the coordinated ligand can be expected in the position of cleavage, since the sterical and electronical influences of an metal ion cannot be considered in this work.

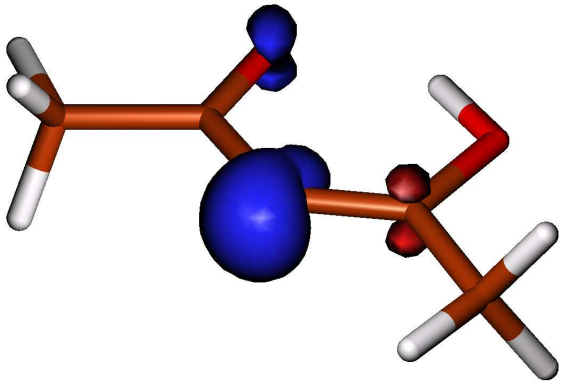

Figure 3.5: Spin density plot of the acetylacetone radical

Part IV

Conclusions

The aim of this work was the formation and theoretical investigation of inorganic-organic hybrid materials based on bidentate β-dicarbonyl ligands and furthermore the theoretical investigation of initiators used in ATRP reactions. The three ligands 2,3-diacetylhexane-2,5-dione, 2,3-dibenzoyl-1,4-diphenylbutane-1,4-dione and tetramethylethan-1,1,2,2-tetracarboxylate were synthesized and characterized using various spectroscopic methods. It was found that the three ligands are present in different tautomer forms. While 2,3-dibenzoyl-1,4-diphenylbutane-1,4-dione and tetramethylethan-1,1,2,2-tetracarboxylate were found as dimer dicarbonyls 2,3-diacetylhexane-2,5-dione is stabilized by dual enolization. The experimental results could be confirmed by DFT calculations. The geometries were optimized and spectroscopic data predicted. Furthermore theoretical considerations were carried out on model complexes containing 2,3-diacetylhexane-2,5-dione to obtain information how the coordination to metal ions occur. This allowed to choose a variety of metal ions usable for coordination reactions forming structured networks. The same ligand was used as sample system for calculations based on periodic boundary conditions - initially derived in solid state physics - showing much better time to quality ratios. The gained data showed good correlations to the experimental and calculated data, which were based on molecular orbitals theory using Gaussian type orbitals. This allowed the study of simplified systems formed by the coordination of the ligand 2,3-diacetylhexane-2,5-dione to metal ions. The investigated coordination systems were based on aluminium, yttrium and copper. Although the different attempts of forming structured metal-organic systems failed, the formation of coordinated substructures could be verified by comparison of solid state IR spectra to the predicted data derived from the simplified systems. The investigated systems were aluminium and yttrium. In the case of copper this could not be carried out due to the disability to derive an adequate pseudopotential which lead to non converging wave functions.

Another part of this work dealed with theoretical studies carried out on different ATRP initiators. The investigations carried out focused on the necessary energy of cleavage of the halide atom from the remaining radical, which is the basic and rate determining step for polymerization. Two different types

of initiators were discussed. One group are the applied and therefore well characterized and investigated compounds for conventional ATRP, which are the molecules and respective radicals of methyl 2-bromopropionate, methyl 2-bromo-2-methylpropionate and 1-phenylethyl bromide. The structures were optimized and vibrational analysis was carried out using DFT calculations. The obtained energies were compared to experimental and theoretical data provided in earlier works showing good correlation. This allowed the use of the applied methods for novel ligands that contain halides usable for the initiation process of ATRP. Investigations on both types of initiators were carried out for determination of the local spin densities of the radicals, which allow a prediction of the initiating step. In all cases the maximum spin densities could be found in the position where cleavage occurred. This work offered a new insight into the possibilities of formation and characterization of novel β-diketone based ligands and their application to form structured metal-organic hybrid materials.

Part V

Experimental Section

General Procedures

5.1 Measurements

NMR spectra were recorded on a 300 MHz DRX Avance Bruker instrument working at 300MHz for ^{1}H and 75.5MHz for ^{13}C spectroscopy. IR spectra were recorded on a Bruker Tensor FT-IR spectrometer with a MVP single reflection ATR unit. Single crystal X-Ray Spectroscopy was carried out on a Bruker-AXS SMART diffractometer with an APEX CCD area detector. Graphite-monochromated Mo-K_α radiation (71.073 pm) was used for all measurements. The nominal crystal-to-detector distance was 5.00 cm. A hemisphere of data was collected by a combination of three sets of exposures at 173 K. Each set had a different Φ angle for the crystal, and each exposure took 20 s and covered 0.3° in ω. The data were corrected for polarization and Lorentz effects, and an empirical absorption correction (SADABS [39]) was applied. The cell dimensions were refined with all unique reflections. The structure was solved by direct methods (SHELXS97 [40]). Refinement was carried out with the full-matrix least-squares method based on F2 (SHELXL97 [40]) with anisotropic thermal parameters for all non-hydrogen atoms. Hydrogen atoms were inserted in calculated positions and refined riding with the corresponding atom.

5.2 Materials

All chemicals were obtained by Aldrich and used without further purification. If not additionally mentioned all chemicals were used without further

purification. Diethyl ether was dried over potassium hydroxide and absoluted over natrium in argon atmosphere. Oxygen and humidity sensitive reactions were carried out in an argon atmosphere with Schlenk techniques.

5.3 Calculations

All calculations with GAUSSIAN98 [22] were carried out on a Silicon Graphics CRAY Origin 2000 system. The used basis set was 6-31++g(d,p) and for electron correlation density functional theory was applied with the exchange correlation functional B3LYP. For calculations determining the spin densities of radical systems the used electron correlation method was limited electron interaction. Calculations with CPMD [23] were carried out on a Silicon Graphics CRAY Origin 2000 system and a Compaq SC45 cluster consisting of 11 nodes with 4 Alpha-EV68 processors and 16GB memory each. The used pseudopotentials were David Vanderbilt Ultra Soft Pseudopotentials [36] for geometry optimization and frequency calculations and Goedeckers norm conserving pseudopotentials for the prediction of magnetic shifts. In both cases the used exchange correlation functional was PBE. Frequency calculations were commonly applied to confirm the local minima of the optimized structures.

Dimer β-Diketones

5.4 2,3-Diacetylhexane-2,5-dione

Acetylacetone (25.0g, 250mmol) was added dropwise, over a period of 3 hours under an argon atmosphere, to a diethyl ether slurry (200ml) of sodium hydride (6.0g, 250mmol). Additional 250ml ether were added and the mixture heated so as to extract iodine (31.6g, 125mmol) from a Soxhlet thimble placed below the condenser. On competition of the iodine extraction the mixture was allowed to cool, excess filtered and the solid washed with diethyl ether and water to remove any access iodine present. The resultant white solid was recrystallized from acetic acid. The product recrystallized in white platelets. The obtained yield was 34%. ^{1}H NMR (δ, $CDCl_3$): 2.0 (12H, s, -CH_3), 16.8 (2H, s, -OH); ^{13}C NMR (δ, $CDCl_3$): 23.6 (-CH_3), 108.1 (C(3), C(10)), 192.7 (C=O); ν_{max}/cm^{-1}: O-H: 1255, 1365, 1403, 1576, 3005; lattice: 668, 679, 913; -CH_3: 997, 1015;

5.5 2,3-Dibenzoyl-1,4-diphenylbutane-1,4-dione

Dibenzoylmethane (10.0g, 45mmol) was solved in diethyl ether (50ml) and the thus obtained mixture was added under an argon atmosphere during 3 hours to a stirred suspension of sodium hydride (1.1g, 45mmol) and diethyl ether (35ml). During the addition further diethyl ether (80ml) was added. After the addition was finished additional diethyl ether (100ml) was added and iodine (5.66g,) was extracted form a Soxhlet thimble placed below the condenser. The solution was allowed to cool down and stirred at room tem-

perature for two days. The solid was filtered and washed with ether and water to remove sodium iodide and any access of iodine. The remaining yellow solid was recrystallized in acetic acid. The product recrystallized in beige needles. The obtained yield was 0.5%. ^{1}H NMR (δ, $CDCl_3$): 2.3 (4H, s, C-H), 7.2-7.7 (8H, m, ph), 7.9-8.1 (12H, m, ph); ^{13}C NMR (δ, $CDCl_3$): 93.2 (C-H), 127.2 (ph), 127.5 (ph), 127.9 (ph), 128.2 (ph), 128.7 (ph), 129.0 (ph), 132.5 (C-O), 135.6 (C=O), 185.8 (O-H); ν_{max}/cm^{-1}: C=O: 1656, 1684; 680, 746, 1260, 1286, 1447, 1524, 3100;

5.6 Tetramethylethane-1,1,2,2-tetracarboxylate

Under an argon atmosphere dimethyl malonate (33.03g, 250mmol) was added dropwise to a diethyl ether slurry (450ml) of sodium hydride (6.0g, 250mmol). During the addition further 1000ml ether were added to keep the solution stirrable. Afterwards the mixture was heated and iodine (31.6g, 125mmol) was extracted from a Soxhlet thimble placed below the condenser. On competition of the iodine extraction the mixture was allowed to cool, and the white solid was filtered. The solid washed with ether and water to remove any access of iodine present. The obtained yield were 17,3g (53%). ^{1}H NMR (δ, $CDCl_3$): 3.8 (12H, s, -CH_3), 4.2 (2H, s, C-H); ^{13}C NMR (δ, $CDCl_3$): 51.1 (C-H), 53.2 (-CH_3), 167.5 (-COO-); ν_{max}/cm^{-1}: C=O:1742, 1716, lattice: 1440, 1311, 1270, 1174, 1154, 997, 889;

Ligand-Metal-Ion Systems

5.7 Tris(3,4-diacetylhexane-2,5-dione)aluminium

A solution of aluminiumnitrate nonahydrate (0.47g, 1.91mmol) in 15ml warm ethanol was slowly added to a solution of Sodium-3,4-diacetylhexane-2,5-dione (0.47g, 1.92mmol) in 15ml ethanol. After 10 min stirring at 60°C, the solution was filtered. A white solid formed after one day, which was filtered and the remaining solid dried in vacuo. The obtained yield was 0.0908g.

^{1}H MAS-NMR (δ): 3.0 (wide); ^{13}C MAS-NMR (δ):: 12.2, 16.2, 22.0, 55.7, 179.1; ^{27}Al MAS-NMR (δ): -5.0 (wide); ν_{max}/cm^{-1}: C=O: 1581, lattice: 3500, 1581, 1469, 1355, 1049, 948, Al-O: 676; Elem. Anal. Calcd: C, 55.0; H, 7.7; N 0.0. Found: C, 11.28; H, 1.93; N, 7.76.

5.8 Bis(3,4-diacetylhexane-2,5-dione)copper

5.8.1 Preparation using Copper(II)chloride

3,4-Diacetylhexane-2,5-dione (0.47g, 1.92mmol) and copper(II)chloride dihydrate (0.33g, 1.92mmol) were dissolved in 10ml ethanol respectively and the solutions united afterwards. A blue-green precipitate was formed immediately, which was filtered and dried in vacuo.

ν_{max}/cm^{-1}: lattice: C=O: 1630(s), 1565(s), 3500(s), 3400(s), 2926(w), 1552(s), 1413(s); Elem. Anal. Calcd: C, 45.5; H, 6.1; Found: C, 4.61; H, 1.08.

5.8.2 Preparation using Copper(II)nitrate

3,4-Diacetylhexane-2,5-dione (0.47g, 1.92mmol) and copper(II)nitrate trihydrate (0.66g, 1.92mmol) were dissolved in 10ml ethanol respectively and the solutions were united afterwards under stirring. A blue-green precipitate was formed immediately, which was filtered and dried in vacuo. ν_{max}/cm^{-1}: C=O: 1564(w),lattice: 3600(m), 3500(m), 1418(s), 1323(s), 1046(m), 811(m); Elem. Anal. Calcd: C, 70.4; H, 4.7; Found: C, 1.27; H, 0.82; N, 8.95.

5.9 Tris(3,4-diacetylhexane-2,5-dione)yttrium

5.9.1 Preparation using Acetonitrile as Solvent

3,4-Diacetylhexane-3,5-dione (0.15g, 0.77mmol) and yttrium nitrate (0.29g, 0.77mmol) were each dissolved in hot acetonitrile and united afterwards. Crystals were formed but only of the ligand itself.

Two attempts to form crystals of the ligand metal adduct. Approximately 2ml of the remaining solution were placed in an ammonia containing bootle and another 2ml in a bottle containing NEt_3. A gel was formed in both cases after a few hours. The reaction of the sample with ammonia was to fast to form a homogenous network. The reaction with NEt_3 was much slower and formed a homogenous structure. The obtained gel was dried in vacuo, which resulted in a massive decrease of the volume. The remaining solid could be analyzed using IR spectroscopy. ν_{max}/cm^{-1}: C=O: 1575, 1361, lattice: 3479, 2990, 2712, 2360, 2341, 1305, 1034, 1010;

5.9.2 Preparation using Water as Solvent

3,4-Diacetylhexane-3,5-dione (0.15g, 0.77mmol) and yttrium nitrate (0.29g, 0.77mmol) were separately dissolved in water. The yttrium nitrate solution was filtered and then united with the ligand. Sodium hydrogen phosphate was added until a white precipitate was formed. The solid was filtered and dried in vacuo. Due to insolubility of the obtained solid only IR spectroscopy

could be carried out for analysis. ν_{max}/cm^{-1}: C=O: 1361, lattice: 1073, 1001;

Part VI

Appendix

Bibliography

[1] M. Eddaoudi, D. B. Moler, H. Li, B. Chen, Th. M. Reineke, M O'Keeffe, and O. M. Yaghi. Modular chemistry: Secundary building units as a basis for the design of highly porous and robust metal-organic carboxylate frameworks. *Acc. Chem. Res.*, 34:319–330, 2001.

[2] P.J. Stand and B. Olenyuk. Self-assembly, symmetry, and molecular architecture: Coordination as the motif in the rational design of supramolecular metallacyclic polygons and polyhedra. *Acc. Chem. Res.*, 30:502–518, 1997.

[3] B. Moulton and M.J. Zaworotko. From molecules to crystal engineering: Supramolecular isomerism and polymorphism in network solids. *Chem. Rev.*, 101:1626–1658, 2001.

[4] S.R. Seidel and P.J. Stang. High-symmetry coordination cages via self-assembly. *Acc. Chem. Res.*, 35:972–983, 2002.

[5] W. Clegg, D.R. Harbron, C.D. Homan, P.A. Hunt, I.R. Little, and B.P. Straughan. Crystal structures of three basic zinc carboxylates together with infrared and FAB mass spectroscopy studies in solution. *Inorganica Chimica Acta*, 186:51–60, 1991.

[6] H. Li, M. Eddaoudi, M. O'Keeffe, and O.M. Yaghi. Design and synthesis of an exceptionally stable and highly porous metal-organic framework. *Nature*, 402:276–279, 1999.

[7] M. Al-Hussein, B.G.G. Lohmeijer, U.S. Schubert, and W.H. de Jeu. Melt morphology of polystyrene-poly(ethylene oxide) metallo-supramolecular diblock copolymer. *Macromolecules*, 36:9281–9284, 2003.

[8] T. Salditt, Q. An, A. Plech, J. Peisl, Ch. Eschbaumer, Ch.H. Weidl, and U.S. Schubert. Self-assembled thin films of organo-metal complexes. *Thin Solid Films*, 354:208–214, 1999.

[9] S. Schmatloch and U.S. Schubert. Engineering with metallo-supramolecular polymers: Linear coordination polymers and networks. *Macromol. Symp.*, 199:483–497, 2003.

[10] K. Matyjaszewski and J. Xia. Atom Transfer Radical Polymerization. *Chem. Rev.*, 101:2921–2990, 2001.

[11] T.S.C. Pai, Ch. Barner-Kowollik, Th.P. Davis, and M.H. Stenzel. Synthesis of amphiphilic block copolymers based on poly(dimethylsiloxane) via fragmentation chain transfer (RAFT) polymerization. *Polymer*, 45:4383–4389, 2004.

[12] J.F. Baussard, J.L. Habib-Jiwan, A. Laschewsky, M. Mertoglu, and J. Storsberg. New chain transfer agents for reversible addition-fragmentation chain transfer (RAFT) polymerization in aqueous solution. *Polymer*, 45:3615–3626, 2004.

[13] Y.A. Vasilieva, D.B. Thomas, Ch.W. Scales, and Ch.L. McCormick. Direct controlled polymerization of a cationic methacrylamido monomer in aqueous media via the RAFT process. *Macromolecules*, 37:2728–2737, 2004.

[14] S. Perrier, P. Takolpuckde, J. Westwood, and D.M. Lewis. Versatile chain transfer agents for reversible addition fragmentation chain transfer (RAFT) polymerization to synthesize functional polymeric architectures. *Macromolecules*, 37:2709–2717, 2004.

[15] H. Zhang, K. Hong, and J.W. Mays. First report of nitroxide mediated polymerization in an ionic liquid. *Polymer Bulletin*, 52:9–16, 2004.

[16] Th. Wannemacher, D. Braun, and R. Pfaendner. Novel copolymers via nitroxide mediated controlled free radical polymerization of vinyl chloride. *Macromol. Symp.*, 202:11–23, 2003.

[17] L. Couvreur, C. Lefay, J. Belleney, B. Charleux, O. Guerret, and S. Magnet. First nitroxide-mediated controlled free-radical polymerization of acrylic acid. *Macromolecules*, 36:8260–8267, 2003.

[18] T.E. Patten and K. Matyjaszewski. Atom transfer radical polymerization and the synthesis of polymeric materials. *Adv. Mater.*, 10:901–915, 1998.

[19] D. Holzinger and G. Kickelbick. Modified cubic spherosilicates as macroinitiators for the synthesis of inorganic-organic starlike polymers. *J. Poly. Sci., A*, 40:3858–3872, 2002.

[20] D. Holzinger and G. Kickelbick. Preparation of amorphous metal-oxide-core polymer-shell nonoparticles via a microemulsion-based sol-gel approach. *Chem. Mater.*, 15:4944–4948, 2003.

[21] G. Li, J. Fan, R. Jiang, and Y. Gao. Cross-linking the linear polymeric chains in the ATRP synthesis of iron oxide/polystyrene core/shell nanoparticles. *Chem. Mater.*, 16:1835–1837, 2004.

[22] M. J. Frisch, G. W. Trucks, H. B. Schlegel, G. E. Scuseria, M. A. Robb, J. R. Cheeseman, V. G. Zakrzewski, J. A. Montgomery Jr., R. E. Stratmann, J. C. Burant, S. Dapprich, J. M. Millam, A. D. Daniels, K. N. Kudin, M. C. Strain, O. Farkas, J. Tomasi, V. Barone, M. Cossi, R. Cammi, B. Mennucci, C. Pomelli, C. Adamo, S. Clifford, J. Ochterski, G. A. Petersson, P. Y. Ayala, Q. Cui, K. Morokuma, D. K. Malick, A. D. Rabuck, K. Raghavachari, J. B. Foresman, J. Cioslowski, J. V. Ortiz, A. G. Baboul, B. B. Stefanov, G. Liu, A. Liashenko, P. Piskorz, I. Komaromi, R. Gomperts, R. L. Martin, D. J. Fox, T. Keith, M. A. Al-Laham, C. Y. Peng, A. Nanayakkara, C. Gonzalez, M. Challacombe, P. M. W. Gill, B. Johnson, W. Chen, M. W. Wong, J. L. Andres, C. Gonzalez, M. Head-Gordon, E. S. Replogle, and J. A. Pople. Gaussian 98,

Revision A.7. http://www.gaussian.com. Gaussian, Inc., Pittsburgh PA, 1998.

[23] Michele Parrinello, Jurg Hutter, D. Marx, P. Focher, M. Tuckerman, W. Andreoni, A. Curioni, E. Fois, U. Roetlisberger, P. Giannozzi, T. Deutsch, A. Alavi, D. Sebastiani, A. Laio, J. VandeVondele, A. Seitsonen, and S. Billeter. CPMD, Version 3.7.0. http://www.cpmd.org. IBM Research Division and MPI Festkörperforschung Stuttgart.

[24] L.Y. Cho and J.R. Romero. Chemical and electrochemical oxidative dimerization of carbonyl compounds by cerium(IV) salts. A comparative study. *Tetrahedron Letters*, 36:8757 – 8760, 1995.

[25] P. A. Krueger, B. Moubaraki, G. D. Fallon, and K. S. Murray. Tetranuclear copper(II) complexes incorporating short and long metal-metal separations: Synthesis, structure and magnetism. *J. Chem. Soc., Dalton Trans.*, pages 713 – 718, 2000.

[26] W.L. Mosby. Reactions of some 1:4-dicarbonyl systems with hydrazine. *J. Chem. Soc.*, pages 3997 – 4003, 1957.

[27] R.M. Moriarty, R.K. Vaid, V.T. Ravikumar, B.K. Vaid, and T.E. Hopkins. Hypervalent iodine oxidation: α-Functionalization of β-dicarbonyl compounds using iodosobenzene. *Tetrahedron*, 44:1603 – 1607, 1988.

[28] Sigma-Aldrich. http://www.sigmaaldrich.com.

[29] J.R. Cannon, V.A. Patrick, and A.H. White. The conformation of some 1,1,2,2-tetraacylethanes in the solid-state: Crystal-structures of 1,1,2,2-tetrabenzoylethane, 1,2-diacetyl-1,2-dibenzoylethane and 1,1,2,2-tetraethoxycarbonylethane. *Aust. J. Chem.*, 39:1811 – 1821, 1986.

[30] A. Fernández-Ramos, J. Rodríguez-Otero, M.A. Ríos, and J. Soto. Intramolecular proton transfer in 2-(2'-hydroxyphenyl)benzoxazole: The reliability of ab initio calculations on simplified structures. *Journal of Molecular Structure (Theochem)*, 489:255–262, 1999.

[31] S.S. Turner, D. Collison, F.E. Mabbs, and M. Halliwell. Preparation, magnetic properties and crystal structure of bis[3-(4-pyridyl)pentane-2,4-dionato]copper(II). *J. Chem. Soc., Dalton Trans.*, pages 1117 – 1118, 1997.

[32] J.W. Carmichael, L.K. Steinrauf, and R.L. Belford. Bis(3-phenyl-2,4-pentanedionato). *J. Chem. Phys.*, 43:3959 – 3966, 1965.

[33] I. Robertson and M.R. Truter. The crystal structure of bis-(3-methylpentane-2,4-dionato)copper(II). *J. Chem. Soc.*, A:309 – 313, 1967.

[34] Sans-Lenain and A. Gleizes. Structural features of homo- and heteroleptic complexes of copper(II) with 2,2,6,6-tetramethyl-3,5-heptanedione and 3-chloro-2,4-pentanedione. *Chim. Acta*, 211:67 – 75, 1993.

[35] H.F. Holtclaw and J.P. Collman. Infrared absorption of metal chelate compounds of 1,3-diketones. *J. Am. Chem. Soc.*, 79:3318 – 3322, 1957.

[36] Group of D. Vanderbilt. Vanderbilt Ultra-Soft Pseudopotential Site. http://www.physics.rutgers.edu/%7Edhv/uspp/.

[37] M.B. Gillies, K. Matyjaszewski, P. Norrby, T. Pintauer, R. Poli, and Ph. Richards. A DFT study of R-X bond dissociation enthalpies of relevance to the initiation process of Atom Transfer Radical Polymerization. *Macromolecules*, 36:8551–8559, 2003.

[38] A.V. Marenich and J.E. Boggs. Structural and thermochemical properties of the dydroxymethyl (CH_2OH) radical: A high precision *ab inito* study. *J. Chem. Phys.*, 119:10105–10114, 2003.

[39] G.M. Sheldrick. Sadabs, 1996. University of Göttingen.

[40] G.M. Sheldrick. Shelxs97 and shelxl97, 1997. University of Göttingen.